Ore Geology Reviews 45 (2012) 61–80

Contents lists available at SciVerse ScienceDirect

Ore Geology Reviews

journal homepage: www.elsevier.com/locate/oregeorev

Geochemical indicators of gold-rich zones in the La Josefina epithermal deposit, Deseado Massif, Argentina

Pablo Andrada de Palomera [a,b,*], Frank J.A. van Ruitenbeek [a], Freek D. van der Meer [a], Raúl Fernández [c]

[a] Faculty of Geo-information Science and Earth Observation (ITC), University of Twente, Enschede, The Netherlands
[b] Fomicruz S.E., Alberdi 643, (9400) Rio Gallegos, Santa Cruz, Argentina
[c] Instituto de Recursos Minerales, Calle 64 e/119 y 120 s/n° CP B1904DZB, La Plata, Argentina

ARTICLE INFO

Article history:
Received 14 October 2010
Received in revised form 11 January 2012
Accepted 13 January 2012
Available online 25 January 2012

Keywords:
Epithermal
Geochemistry
Hydrothermal alteration
Weathering
Deseado Massif
Mineral exploration

ABSTRACT

The gold deposit at La Josefina, in the Deseado Massif of Argentina, is a low-sulfidation epithermal deposit with some features of the intermediate sulfidation style; the Au occurs in quartz veins and hydrothermal breccias hosted by acid pyroclastic rocks produced by Jurassic bimodal volcanism. Exploration for this deposit type uses geochemical data for vectoring to mineralized rocks. Although a general suite of elements with anomalous concentrations around low-sulfidation deposits is known, that suite varies amongst individual deposits, which should be studied individually. The aim of this study was to determine, in the La Josefina deposit, geochemical indicators of Au-rich rocks at different scales and to assess the effects of weathering on those indicators. To reach these objectives, a mineralized zone (hosting Au-rich veins) and a non-mineralized zone (hosting barren veins) were compared in terms of vein mineralogy, alteration minerals and geochemistry. These zones were also compared with estimated element concentrations of the protolith. Element concentrations in the mineralized zone were then plotted against distance to the Au-rich veins, separating the dataset into two subsets: one from strongly oxidized rocks and the other from weakly oxidized rocks, considering the degree of oxidation as indicative of relative degree of weathering. Based on alteration and vein mineralogy, we interpret that the mineralized zone was hydrothermally active before, during and after Au-mineralization, while the non-mineralized zone was active only before Au-mineralization. Therefore, differences in element concentrations between the estimated protolith and the non-mineralized zone represent geochemical changes produced before mineralization, whereas differences between mineralized and non-mineralized zones represent changes produced during and after mineralization. We conclude that in rhyolitic to rhyodacitic pyroclastic rocks of the study area, affected by predominantly argillic and silicic hydrothermal alterations, high concentrations of Au, Cu, Hg, V, Co and P, and low concentrations of Ba are probably the best deposit-scale geochemical indicators to distinguish Au-mineralized zones from non-mineralized zones. High concentrations of As, Mn, Fe, Pb, Cr, Ni, MgO and Zn (as well as high values of chlorite-carbonate-pyrite index), and low concentrations of Be and CaO can also distinguish mineralized from non-mineralized zones. High concentrations of Au, Cu, Pb, As, Hg, and Co indicate Au-rich zones, independently of lithology and alteration, because they were introduced into the veins and host rocks together with Au. At detailed-scale, the concentrations of 15 elements vary with distance to Au-rich veins; therefore, those elements are considered potential indicators of proximity to Au-rich veins. Of those elements, Au, P, Cu, Pb, Hg, Ba and MgO are the strongest indicators of proximity to the Au-rich veins. In strongly oxidized rocks, some indicators of mineralized zones (Co, Mn, Pb, Zn and MgO) and some indicators of proximity to Au-rich veins (P, Au, Cu, Hg and Ba) should be used with caution or be avoided because weathering modifies their quality as indicators.

1. Introduction

The Deseado Massif, in the south of Argentina (Fig. 1), is a geological and metallogenic province (Schalamuk et al., 1999), which is recognized as a valuable region for gold exploration. Most of the Au in this province is hosted in low-sulfidation epithermal deposits (Schalamuk et al., 1998; Schalamuk et al., 2002), although some of them exhibit features of the intermediate-sulfidation style (Cedillo Frey et al., 2009; Echavarría et al., 2005; Gonzalez Guillot et al., 2004; Jovic et al., 2004; Moreira et al., 2004a). Several of the Au deposits in the Deseado Massif, including the La Josefina epithermal low-sulfidation deposit, are currently under exploration using abundant geochemical data.

Surface geochemical data are used to interpret and map near-surface Au-rich zones with possible extensions at depth. Subsequently, subsurface geochemistry is used to confirm the presence and size

* Corresponding author at: Faculty of Geo-information Science and Earth Observation (ITC), University of Twente, Enschede, The Netherlands. Tel.: +31 654324614; fax: +31 53 4874336.
E-mail addresses: andradadepalomera@itc.nl, pandrada@fomicruz.com (P. Andrada de Palomera).

0169-1368/$ – see front matter © 2012 Elsevier B.V. All rights reserved.
doi:10.1016/j.oregeorev.2012.01.001

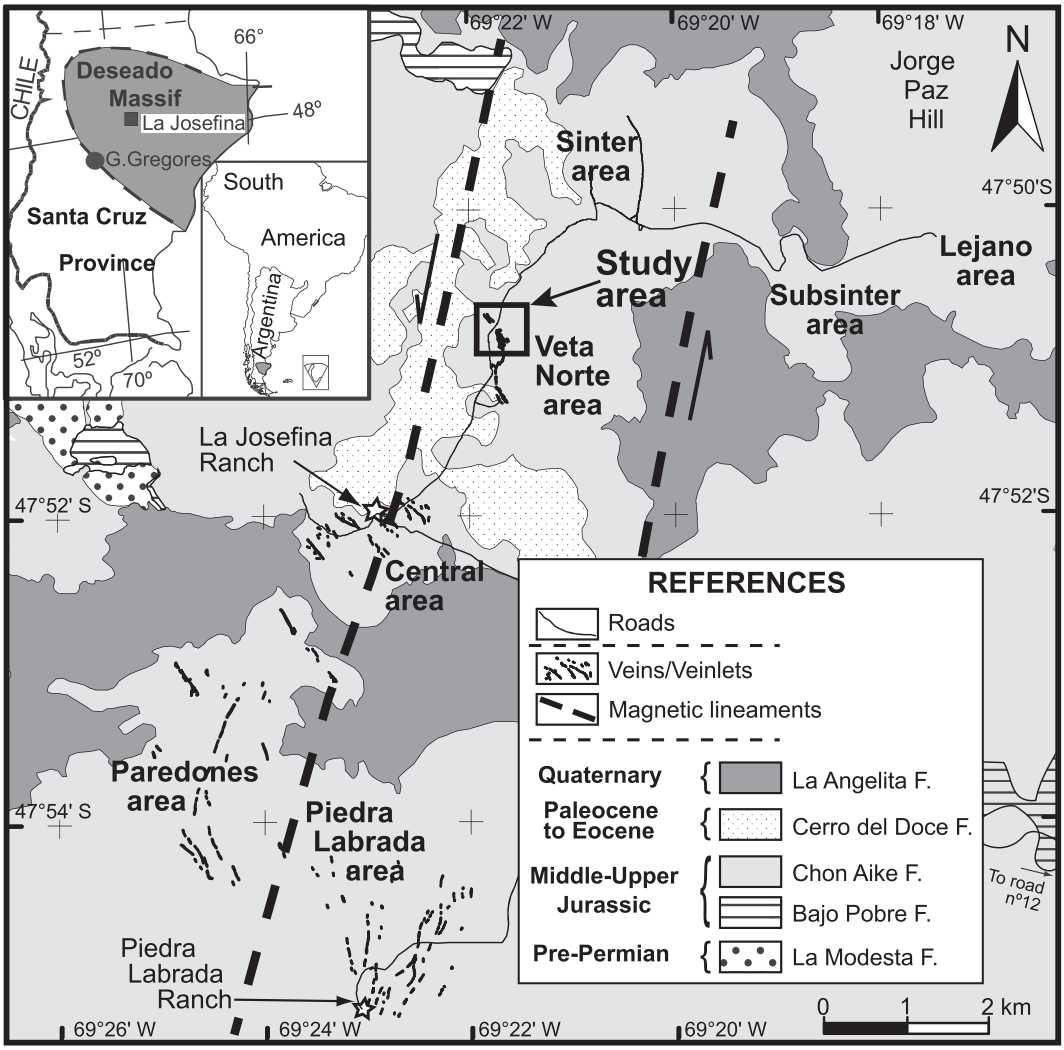

Fig. 1. Location and general geology of the La Josefina deposit. Lithology modified from Moreira (2005). Magnetic lineaments extracted from Peñalva et al. (2005).

of the Au-rich zones at different depths. The Au in these zones usually occurs in breccias and veins, which are mainly composed of quartz and minor adularia, calcite, barite and sulfides. Some mineralized veins and breccias are small or covered by debris and, thus, difficult to detect at the surface. In these cases, geochemical haloes around veins can be used over areas of few hundreds of metres wide (deposit-scale) to indicate the presence and location of mineralized veins. If mineralized veins are detected at the surface or their presence at depth is inferred, areas of tens of metres wide (detailed-scale) around veins are investigated by drilling. The aim of drilling is to cross the mineralized veins at different vertical levels; but often, drilling fails in finding the veins at the expected depths because they either pinched-out or were displaced by faults. However, the drillhole lithogeochemical data can help to determine if veins may be located nearby or if that is unlikely.

For any one of the above-mentioned applications of geochemical data in the Deseado Massif, variations of element concentrations around mineralized rocks should be well known. Such variations in element concentrations have been studied in several low-sulfidation deposits (Berger and Silberman, 1985; John et al., 2003; Mauk and Simpson, 2007; Murakami and Feebrey, 2001; Silberman and Berger, 1985; Warren et al., 2007) and general guidelines have been summarized for such deposits (Cooke and Simmons, 2000; Hayba et al., 1985; Hedenquist et al., 2000; Pirajno, 1992). However, as pointed out by some authors and due to the high variability of element contents within the epithermal environment (Hedenquist et al., 2000; Silberman and Berger, 1985), it would be very difficult to establish either a generalized element distribution model applicable to every deposit or a suite of elements that is always anomalous. Therefore, each deposit or district should be studied separately to know which elements to use and how to use them during exploration.

The geochemical indicators of mineralized zones at deposit-scale in the La Josefina and similar deposits in the Deseado Massif are not well known, and variations in element concentrations at detailed-scale in particular are poorly known elsewhere. In addition, if geochemical data are obtained at or close to the ground surface, the likely effects of weathering on element distribution patterns around mineral deposits should be known. This issue is usually overlooked during exploration, but is essential for proper interpretation of exploration geochemical data. The effects of chemical weathering on primary element dispersion patterns around mineral deposits are unknown in the Deseado Massif. Several researchers (e.g., Duzgoren-Aydin and Aydin, 2009; Duzgoren-Aydin et al., 2002; Malpas et al., 2001; Scott, 2001) studied the effects of chemical weathering, but only in areas not related to mineral deposits or with deposits and climatic conditions different to those in the Deseado Massif.

This study, carried out in the Veta Norte area of the La Josefina deposit (Fig. 1), had three objectives. The first was to determine geochemical indicators that can be used to distinguish deposit-scale

hydrothermally altered zones hosting Au-rich veins. The general approach used for this objective was to find out the modifications that different hydrothermal alterations produced on the lithogeochemistry, particularly those modifications produced during Au-mineralization. The second objective was to determine geochemical indicators that can be used to estimate proximity to Au-rich veins. For this, we studied detailed-scale variations of element concentrations with proximity to Au-rich veins. The third objective was to find out the effects of chemical weathering on element concentrations, to assess the usefulness of geochemical data extracted from the upper parts of the ground profiles. For this, we compared element concentrations at different depths but at a constant distance from Au-rich veins. The results of this study can increase the efficiency of geochemical surveys for mineral exploration in the La Josefina and similar deposits.

2. Regional geology

The oldest rocks in the western part of the Deseado Massif are pre-Permian low-grade metamorphic rocks of the La Modesta Formation. Those rocks are covered by a sequence of intra-continental sedimentary rocks including a Lower Permian syn-extensional rift sequence of the La Golondrina and La Juanita Formations and a Triassic to Early Jurassic sag sequence of the El Tranquilo and Roca Blanca Formations (Giacosa et al., 2010).

During the Middle to Late Jurassic, a generalized extension produced the break-up of Gondwana and the opening of the South Atlantic Ocean, generating a series of NNW-trending half-grabens (Ramos, 2002). These events occurred simultaneously with subduction in the western margin of the southern South America (Echavarría et al., 2005). The extensional tectonism and concomitant subduction resulted in volcanism, which filled the NNW-trending grabens with thick volcanic sequences. These volcanic sequences, which are present in Argentina, Chile and probably Antarctica (Pankhurst et al., 1998), constitute the Chon Aike Siliceous Large Igneous Province.

The Jurassic volcanism produced a bimodal volcanic suite of rocks. A minor proportion of the volcanic suite is composed of rocks of the Bajo Pobre and Cerro Leon Formations, which are mainly andesitic in composition (Panza and Haller, 2002) and represent a syn-rift stage (Giacosa et al., 2010). In the Bajo Pobre Formation, the predominant rocks are lavas, but there are minor ash flow tuffs and volcanic agglomerates. The Cerro Leon Formation consists of subvolcanic intrusions, which are likely intrusive equivalents of the Bajo Pobre Formation (de Barrio et al., 1999; Jovic et al., 2011). A major proportion of the volcanic suite is composed of late-rift deposits. These deposits are predominantly ignimbrites and minor fall tuffs and lava flows of the Chon Aike and La Matilde Formations, which are mainly rhyolitic and subordinately dacitic in composition (Panza and Haller, 2002).

The Jurassic volcanic rocks are overlain by the Cretaceous Bajo Grande and Baquero Formations. The Bajo Grande Formation, of Barremian age (Panza, 1998), is composed of conglomerates, sandstones and tuffites deposited in alluvial and lacustrine environments during a post-rift thermal subsidence. The Baquero Formation, of Aptian age (Corbella, 2005), is composed of tuffs and sandstones deposited during a sag phase (Giacosa et al., 2010). During the Cenozoic, several generations of basaltic flows covered the older rocks. From older to younger, they are Las Mercedes basalts of 63–64 Ma, Cerro del Doce basalts of 40–60 Ma, Alma Gaucha basalts of 23–30 Ma (Panza and Franchi, 2002) and finally, Quaternary basalts from the La Angelita Formation.

3. Geology of the study area

Rocks of the La Modesta and Bajo Pobre Formations are located at ca. 4 km to the W and WSW of the study area (Fig. 1). The Bajo Pobre Formation is also present at ca. 2 km to the N. Lava flows of the Cerro del Doce basalts and the La Angelita Formation cover large portions of the La Josefina district (Fig. 1). However, the predominant formation in the district, and the only one outcropping in the study area, is the Chon Aike Formation (Fig. 1).

The Chon Aike Formation in the study area includes several volcanic lithofacies of similar mineralogical compositions. This formation is mainly composed of ignimbrites, consisting of quartz, sanidine, plagioclase and biotite. In the basal part of the formation, there are crystal-rich ignimbrites with an average of 20% crystals of quartz, sanidine, plagioclase and biotite, and locally with fiammes (Moreira, 2005). Over these rocks, there are lithic and pumice-rich ignimbrites with abundant matrix and fiammes, showing moderate to high degree of welding (Moreira, 2005). Intercalated with the ignimbrites are scarce layers of laminated fine-grained fall tuffs and reworked volcaniclastic rocks; those layers are <1 m thick and are composed of quartz, plagioclase, sanidine and biotite. In addition, there are clast-supported volcanic breccias with fragments of up to 40 cm composed of acid lavas and crystal-rich ignimbrites. These breccias have a light grey matrix with lithic and pumice fragments of up to 5 mm. The Chon Aike Formation includes also lava flows outcropping a few hundred metres to the west outside the study area. Some fragments of the mentioned breccias may have come from these lavas. The lavas have aphanitic textures and less than 10% of microphenocrysts (Moreira, 2005); their groundmass is composed of quartz, potassic feldspars and scarce plagioclase and their phenocrysts are mainly plagioclase, biotite and scarce quartz and sanidine. Moreira (2005) mentioned the presence of lavas in the northern part of the study area, although these rocks have not been detected in trenches and boreholes drilled there.

The development of the vein system in the La Josefina epithermal deposit was strongly structurally controlled. The controlling structures were two main fractures of NNE orientation, one of which is located at ca. 300 m to the west of the study area (Fig. 1). The locations of these two main fractures were inferred from the interpretation of two regional aeromagnetic lineaments (Peñalva et al., 2005). These two lineaments were interpreted as part of a shear zone with sinistral displacements produced by a principal stress ($\sigma 1$) directed at ca. 340° and an extensional direction ($\sigma 3$) with azimuth of 70–80° (Moreira et al., 2008). Within this framework of stress and under the Jurassic general extensional environment, NNW trending veins were developed in dextral-slip faults (Moreira et al., 2008). Those veins were later dissected by WNW trending dextral-slip faults.

4. Mineralization in the study area

Most features of the La Josefina deposit are of the low-sulfidation epithermal style (Rios et al., 2000; Schalamuk et al., 1998). The minerals of economic significance include Au and Ag, which are contained in quartz veins, veinlets and hydrothermal breccias that often include adularia. The veins include mainly open-space textures, predominantly comb and saccharoidal, but also colloform–crustiform and bladed textures. Other typical features of low-sulfidation deposits present in La Josefina are siliceous and calcareous sinter deposits. However, the common barite in the veins, the salinity of fluid inclusions reaching 15 wt.% NaCl eq. (Rios et al., 2000) and the FeS content of sphalerite from 2.72 to 5.2 mol% (Moreira et al., 2004a) are probably more typical features of intermediate-sulfidation deposits.

The Au–Ag-rich veins and related hydrothermal alterations at La Josefina are genetically related to the Jurassic volcanism. The ages of the Jurassic Chon Aike Formation, 153 ± 3.6 Ma to 148.8 ± 3.6 Ma (Arribas et al., 1996; Moreira et al., 2009), and the age of the hydrothermal alterations (156 ± 2 Ma) may overlap (Fernández et al., 1999). This temporal overlap is inferred from the positions of veins in the volcanic sequence of the Chon Aike Formation. Most of the veins and veinlets are hosted in the older units of the Chon Aike Formation, while siliceous and calcareous deposits, interpreted as the

upper part of the epithermal paleo-system, seem to rest below the youngest units of this formation. This implies that the La Josefina hydrothermal system was temporally constrained in the Chon Aike Formation. The similar Pb isotopes ratios calculated for the volcanic rocks and for sulfides in the epithermal veins also indicate a genetic link between the Jurassic volcanic rocks and the mineralization (Moreira et al., 2005).

Different areas in the La Josefina deposit represent different levels of an epithermal paleo-system. The Veta Norte, Central, Paredones and Piedra Labrada areas (Fig. 1) are interpreted as relatively deep levels of the paleo-system because they include veins of predominantly coarse crystalline quartz, some calcite and adularia, and the temperatures of homogenization in fluid inclusions reach up to 290 °C. In contrast, the Sinter, Subsinter and Lejano areas (Fig. 1) are interpreted as the upper levels of the paleo-system. In the last three areas, quartz veinlets are scarce and there are siliceous and calcareous deposits interpreted as evidence of paleo-surface (Moreira et al., 2002b). Pervasive silicification and abundant kaolinite, typically produced by steam-heated waters in the upper parts of epithermal paleo-systems, are also present in the Sinter, Subsinter and Lejano areas.

In the Veta Norte area, the Au-mineralization is associated mainly with NNW trending quartz veins. These veins are located along a NNW–SSE trending zone measuring ca. 200 m wide and more than 1300 m long. In this zone, the activity of faults during the Jurassic, coupled with inflections along them, favoured the formation of the quartz veins and hydrothermal breccias in sectors with local extension, but hindered their formation in sectors with local compression. Thus, the veins are discontinuous, both at the surface and in the subsurface, and show variable widths and directions. These observations support the interpretations of Moreira et al. (2008) about the presence of several WNW–ESE syn-mineralization fractures (Fig. 2) and the likely arrangement of fractures and veins at depth, which are discontinuous.

The study area is located in the northern part of the Veta Norte area, which includes the Flaca East, Flaca West, Amanda and Cecilia veins (Fig. 2). The Flaca East and West (FEW) veins are parallel and ca. 30 m apart. They have thicknesses of up to 0.3 m, strikes of 310–330° and dips of almost 80° to the ENE. The FEW veins are hosted in volcanic breccias of the Chon Aike Formation. The Amanda and Cecilia (AC) veins are composed of several sub-parallel veins, veinlets and hydrothermal breccias. They have variable thicknesses, reaching occasionally 3 m. They have strikes of 315–335° and dips of 60–90° to the ENE, although some veinlets dip ca. 70° to the WSW. The AC veins are hosted by lithic and pumice-rich ignimbrites, crystal-rich ignimbrites and volcanic breccias of the Chon Aike Formation.

In the AC veins, the predominant gangue minerals are quartz and chalcedony, but there is minor adularia, barite, opal and calcite. In the Central area (Fig. 1), rhombic adularia, probably contemporary with Au precipitation, yielded temperatures of homogenization of 250–270 °C and salinity of 4.6 wt.% NaCl eq. (Moreira, 2005). In the

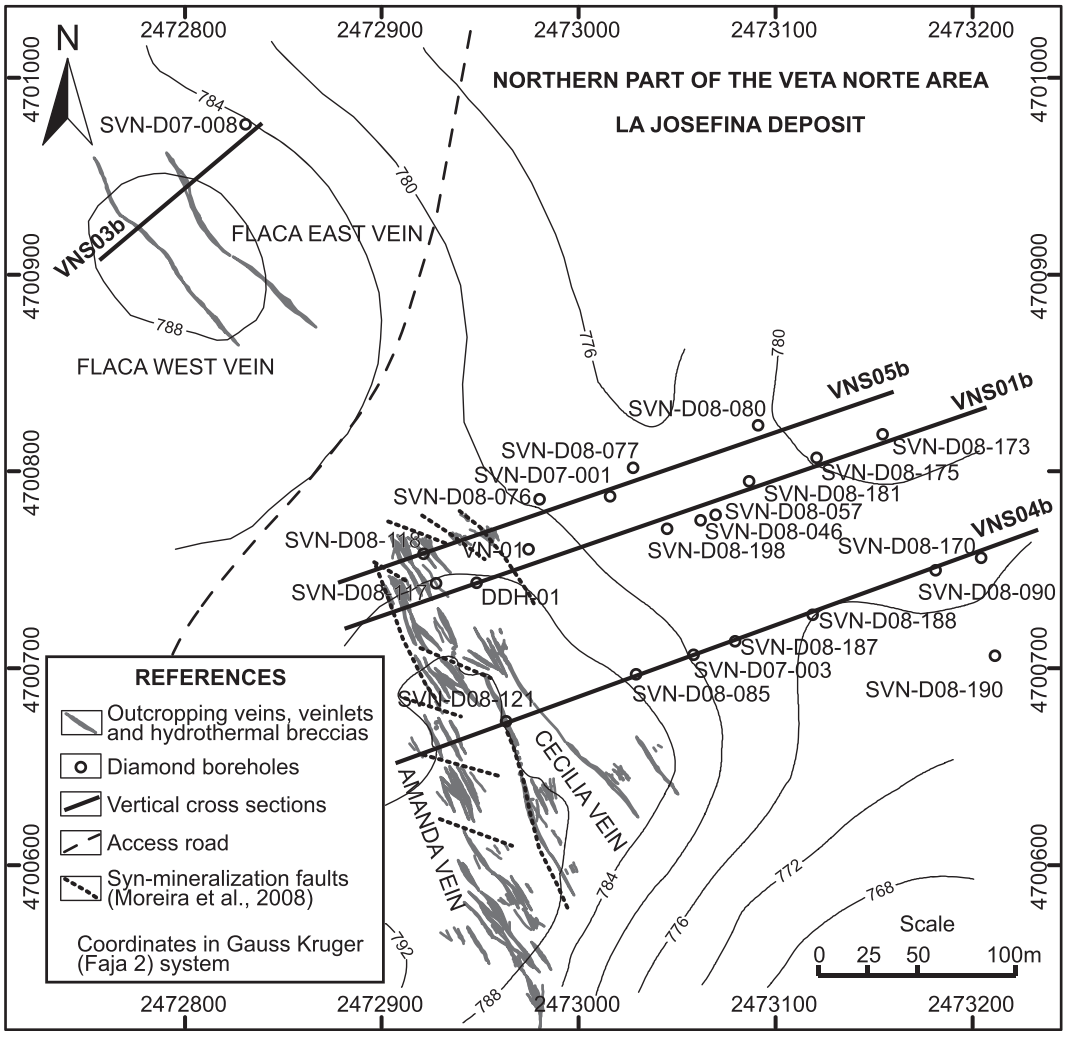

Fig. 2. Map of the study area in the northern portion of the Veta Norte area. Boreholes were drilled sub-parallel to the cross sections, towards SW.

AC veins, adularia was identified at 75 m vertical depth in borehole SVN-D08-198 and at more than 250 m vertical depth in borehole SVN-D08-190 (Fig. 2). In several veins and veinlets, adularia coexists with comb quartz, banded quartz, pyrite and chalcopyrite. Barite mainly occurs in the centre of the AC veins and is often replaced by opal or chalcedony, forming lattice-bladed textures. It is also present in fragments of some breccias cemented with opal and iron oxides. Barite was considered a relatively late mineral, deposited at less than 100 °C and crystallized from a fluid with salinity of 4–5 wt.% NaCl eq. (Rios et al., 2000).

In the AC veins, the ore minerals are mainly native Au, electrum and silver sulfosalts. Native Au occurs as irregular grains in quartz with saccharoidal and comb textures, or as inclusions in oxidized pyrite or disseminated in iron oxides filling fractures. Gold grains have a mean composition of 80.6% Au, 18.5% Ag, and traces of Bi, Te, and As (Schalamuk et al., 1998). Some of the observed Au may have been dissolved and re-deposited by supergene processes (Moreira, 2005; Schalamuk et al., 1998). The Au grains frequently show zonation with yellower colour (higher gold purity) towards their boundaries, suggesting the mobilization of Ag after partial dissolution of Au grains (Schalamuk et al., 1998). Electrum occurs mostly in coarse quartz; it has no zonation and has concentrations of 48–60% of Au and 40–52% of Ag (Schalamuk et al., 1998).

Pyrite, galena, chalcopyrite, tetrahedrite, sphalerite, bornite and hematite are also present in the AC veins. Pyrite is the most abundant and widespread sulfide; it occurs abundantly as fillings in the AC and FEW veins and as disseminations in the host rocks. Galena is the most abundant base metal sulfide, and it contains up to 0.03 wt.% Se, up to 0.18 wt.% Ag, 0.08 wt.% Cu, 0.13 wt.% Cd and 0.05 wt.% Au (Schalamuk et al., 1998). Chalcopyrite contains up to 0.01 wt.% Se, some Te, traces of Ag and Sb, and 0.04 wt.% Au (Schalamuk et al., 1998). Tetrahedrite was identified as inclusions in pyrite, galena and sphalerite (Moreira, 2005). Sphalerite is in association with pyrite and in paragenesis with galena and chalcopyrite (Moreira et al., 2004a). Fluid inclusions in sphalerite of the AC veins showed salinities of 1.7–3.4 wt.% NaCl eq. and homogenization temperatures of 190–200 °C (Moreira et al., 2004a). The FeS content in sphalerite varies from 2.72 to 5.21 FeS mol% (Moreira et al., 2004a).

Rios et al. (2000) re-interpreted a paragenetic sequence published by Schalamuk et al. (1998). In this reinterpretation, there are three stages (Fig. 3). The "initial stage" and the "main stage" are hypogene, in contrast to a "supergene" third stage. Adularia was probably the first mineral deposited in the sequence. According to Schalamuk et al. (1998), Au was likely deposited from the end of the initial stage but mainly during the main stage and was later re-mobilized and concentrated during the supergene stage, resulting in high local Au concentrations. Rios et al. (2000) showed that barite precipitated at the end of the main stage, which is consistent with its occurrence in the veins as a late filling material; but those authors also showed that the precipitations of adularia and specularite did not overlap with that of Au. This contrasts with (a) the interpretations of Moreira (2005) that the precipitations of adularia and Au were likely contemporaneous, and with (b) the observations that the specularite is often associated with native Au and high Au contents (Moreira, 2005; Moreira et al., 2004a). Moreover, adularia is often considered as an indication of boiling, which was interpreted as the most likely cause of Au precipitation in the La Josefina deposit (Moreira, 2005; Rios et al., 2000). Therefore, in this research, we adopted a paragenetic sequence modified from that of Rios et al. (2000) considering that precipitations of adularia, Au and sphalerite were partly contemporaneous (Fig. 3) (cf. Schalamuk et al., 1998).

In the AC veins, Moreira (2005) recognized seven types of "vein fillings" but their temporal relationships are unknown. Those types of vein fillings are: (1) quartz with colloform banded, saccharoidal and comb textures, abundant pyrite, and some chalcopyrite, bornite, galena and sphalerite; (2) quartz with colloform banded and saccharoidal textures, banded red opal, and clays; (3) abundant comb quartz (partly amethyst), scarce coarse saccharoidal quartz, some adularia, calcite, native gold, pyrite, chalcopyrite, bornite, specularite, galena, sphalerite, tetrahedrite and silver minerals; (4) veinlets of barite and comb quartz; (5) coarse comb quartz; (6) breccias with opal and oxides of Fe and Mn; and (7) veinlets of coarse comb quartz with up to 90% sulfides, including pyrite, galena, sphalerite and chalcopyrite.

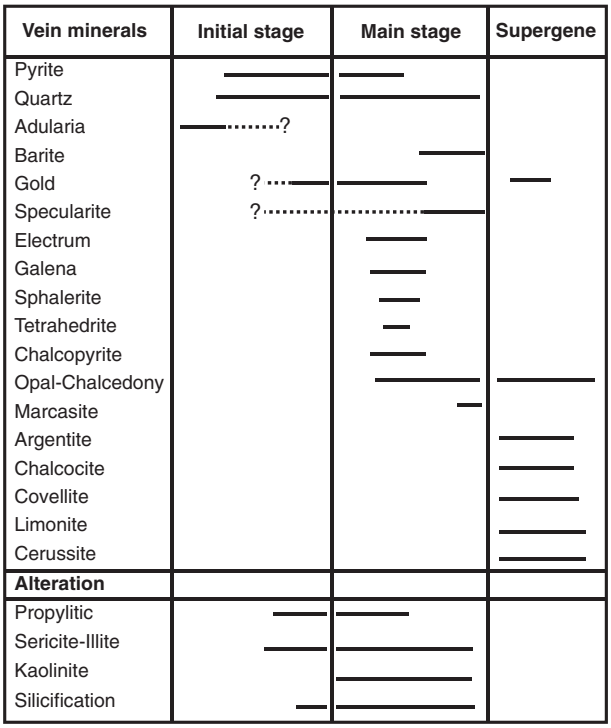

Fig. 3. Paragenetic sequence of the La Josefina deposit (modified from Rios et al., 2000).

In the FEW veins, Moreira (2005) recognized a single type of vein filling (at ground surface level) composed of comb and saccharoidal quartz, some specularite and pyrite, abundant rhombic adularia along the contact with the host rocks, and probably native Au. Although not present as vein filling at ground surface level, scarce calcite veinlets were observed in the subsurface.

The characteristics of vein fillings in the AC and FEW veins suggest that the FEW veins were likely coeval with one of the earliest hydrothermal events observed in the AC veins. Because of their similar quartz textures and mineralogy (including adularia), the vein fillings of the FEW veins are probably temporally correlated with some of type (3) vein fillings of the AC veins, excluding chalcopyrite, bornite, galena, sphalerite, tetrahedrite and silver minerals. Furthermore, the presence of adularia, which is an early mineral (Rios et al., 2000; Schalamuk et al., 1998), suggests that the FEW veins and the type (3) vein fillings in the AC veins were formed during the early stages of formation of the system of veins.

Some general physico-chemical conditions during the formation of type (3) vein fillings in the AC veins can be inferred from data on fluid inclusions in adularia and sphalerite. Those vein fillings were, at least partially, deposited at about 250–270 °C from fluids with salinities of ca. 4.6 wt.% NaCl eq. The fluid salinities, the FeS content in sphalerite, with a mean value of 4.93 mol% (Moreira et al., 2002a), and the presence of tetrahedrite suggest that the type (3) vein fillings, and probably the native Au, were deposited from an intermediate sulfidation fluid.

Types (4) and (6) vein fillings in the AC veins were deposited during the latest stages of the formation of veins. Type (4) vein fillings were likely formed at <100 °C and salinities of 4–5 wt.% NaCl eq., which were the conditions prevailing during the precipitation of

barite in the centre of the veins as a late stage mineral. However, there was possibly at least one later stage of vein fillings because barite was replaced by low temperature silica and was observed in fragments of breccias cemented with opal, chalcedony and iron oxides. Type (6) vein fillings possibly represent this later stage. In the Piedra Labrada area, barite and red opal were found at a late stage; both were described as cement of breccias formed by fracturing of a vein filling with saccharoidal quartz, pseudomorphs of calcite and oxides of Fe and Mn (Moreira, 2005). The other vein fillings described for the AC veins must have formed between the deposition of adularia and that of barite.

5. Methods

In this study, a geological framework for geochemical data analysis and interpretation was established using information from literature and from descriptions of 21 diamond drill cores. The literature was used to establish the general characteristics of the La Josefina deposit and especially those of the study area. The descriptions of the drill cores were used to delineate the location of hydrothermal veins and breccias, to determine the predominant types of hydrothermal alterations, and to represent veins and alterations in four vertical cross sections (VNS01b, VNS03b, VNS04b and VNS05b), which are parallel to the directions of the drillholes (Fig. 2). After setting up the geological framework, geochemical data from the same 21 drill cores were studied, first at deposit-scale (few hundred metres) and then at detailed-scale (tens of metres). Geochemical data from published literature were used to represent the composition of the original fresh rocks; we referred to those fresh rocks as "estimated protolith" (EP).

5.1. Geochemical data

The geochemical data include assays of samples from the drill cores. The drill cores were split in two halves with a diamond saw, and one of the halves was sampled at intervals of 0.3–2 m length (average of 1 m). The length of the sampled intervals was adjusted to obtain a homogeneous core sample. When possible, veins were sampled separately from their host rocks. For calculations involved in analyses of the data (see below), we represented every sample as a point at the centre of the sampled interval.

The samples were analysed for 28 elements using different techniques. ALS-Chemex laboratories determined the concentrations of Au by fire assay, Hg by an aqua regia digestion followed by cold vapour-AAS, and the remaining elements by ICP after digestion with four acids (HF, HNO_3, $HClO_4$, and HCl). Samples with more than 100 ppm Ag or more than 5 ppm Au were re-analysed for those elements with a gravimetric method. The samples from drillhole DDH-01 and most of the samples from drillhole VN-01 were analysed by Fomicuz S.E. for Au only, using aqua regia and methyl isobutyl ketone (MIBK) extraction. Because the digestion and limit of detection of this method is different from that of the fire assay, the concentrations determined by it were used to indicate the presence of mineralized rocks but not for statistical calculations.

Concentrations of minor and trace elements in the "estimated protolith" (EP) were represented by global average abundances in granites, reported by Levinson (1974), while concentrations of P, Mn and major elements were represented by median concentrations calculated from 28 samples of fresh rhyolitic and rhyodacitic ignimbrites of the Chon Aike Formation, collected near the study area by Alperin et al. (2007).

In addition to the individual elements, the K_2O/Na_2O ratio, the alteration index (AI) of Ishikawa et al. (1976) and the chlorite-carbonate-pyrite index (CCPI) of Large et al. (2001) were calculated. The AI $(100(MgO + K_2O)/(MgO + K_2O + CaO + Na_2O))$ indicates the breakdown of sodic plagioclase and volcanic glass and their replacement by sericite and chlorite, through losses of Na and Ca and gains in K and Mg. An increase in CCPI $(100(MgO + FeO)/(MgO + FeO + K_2O + Na_2O))$ may indicate the formation of chlorite, Mg-Fe carbonates, pyrite, magnetite or hematite (Large et al., 2001).

The K_2O/Na_2O, AI and CCPI were used for two objectives. The first objective was to verify that the 28 samples from Alperin et al. (2007), used for calculating concentrations in the EP, represented fresh rocks. The calculated values of K_2O/Na_2O, AI and CCPI for each of those samples are within the ranges for unaltered rhyolitic–dacitic rocks, which are of <2.5 for K_2O/Na_2O (Páez et al., 2010), 20–60 for AI and 10–60 for CCPI (Gifkins et al., 2005; Large et al., 2001). The second objective was to test these three variables as possible geochemical indicators of proximity to mineralized rocks.

5.2. Subdivision of datasets

Based on various criteria (i.e., Au contents, degree of oxidation of rocks, predominant hydrothermal alterations, position relative to the system of veins and distance to mineralized paleo-conduits), an initial geochemical dataset of 1426 samples, assayed for 28 elements, was divided into several datasets used for different parts of the research.

Based on overall Au contents, a mineralized zone (MZ) and a non-mineralized zone (NMZ) were distinguished in the study area. The MZ, which includes the Amanda and Cecilia (AC) veins (Fig. 2); shows a Au-rich vertical interval extending from ground surface to at least 250 m depth, with up to 71.1 ppm Au at 120 m depth. The NMZ, which includes the Flaca East and Flaca West (FEW) veins (Fig. 2), shows low Au concentrations, reaching only 0.19 ppm at ground surface and 0.038 ppm in drillholes. In addition, more than 70% of the samples collected in the NMZ yielded Au concentrations of <0.005 ppm, which is the detection limit (DL) for Au. The absence of high Au contents in the NMZ extends from ground surface to at least 50 m vertical depth.

Regarding the degree of oxidation of the rocks, the vertical interval in which the sulfides (predominantly pyrite) have been completely destroyed and which has abundant Fe-oxides or oxyhydroxides was considered an interval of strong oxidation. This interval has its base at 750 m above sea level (Fig. 4) and extends upwards, for 25–30 m, up to the ground surface. Rocks in the interval of strong oxidation were classified as "strongly oxidized", while those located below were classified as "weakly oxidized". Because oxidation is one of the processes that contribute to chemical weathering, the degree of oxidation was considered a proxy for the degree of weathering. It was not possible to estimate the absolute degree of weathering and its maximum depth because of the lack of specific studies.

Considering the predominant types of hydrothermal alteration of the rocks in the MZ, samples located in the footwall of the system of veins were discarded because hydrothermal alterations in that sector are different from those in the system of veins and its hanging wall, and thus their geochemistry is expected to be different. The small number of samples in the footwall prevented their evaluation as a separate group. The samples from the NMZ were used irrespective of their location relative to the veins because the same types of alteration predominate in the whole cross section.

For the distance to mineralized paleo-conduits criterion, quartz veinlets, siliceous hydrothermal breccias and sulfide veinlets with Au concentrations >0.5 ppm were interpreted as "mineralized paleo-conduits" (MPCs) of epithermal fluids. They were traced in each cross section based on the descriptions of the drill cores. Then, the distance from each sample to the nearest MPC in every cross section was calculated using 10 m wide buffer polygons generated around and perpendicular to the borders of the MPCs (Fig. 4). Only samples up to 60 m from the MPCs were used because the samples in more distant intervals were scarce. In addition, 32 samples located in the deeper part of borehole SVN-D07-001 were discarded

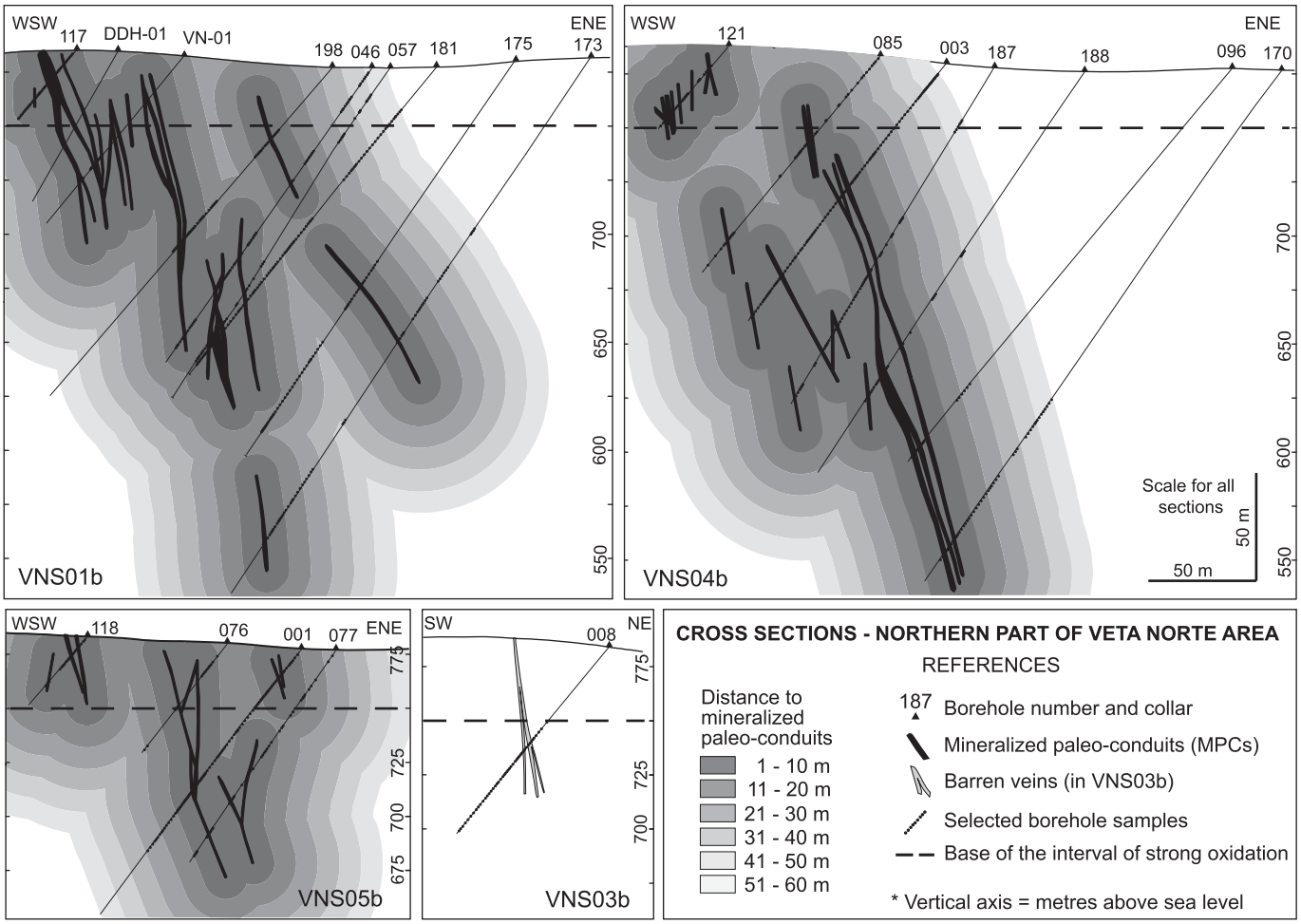

Fig. 4. Vertical cross sections of the mineralized zone (VNS01b/04b/05b) and non-mineralized zone (VNS03b) showing the drillcore samples used during this research and buffers at every 10 m from mineralized paleo-conduits.

because their positions relative to mineralized veins were uncertain; there may be mineralized veins a few metres beyond the end of that borehole.

5.3. Statistical treatment of the geochemical data

Because the concentrations of several elements in some subsets of data show asymmetric distributions, which cannot be adequately described by the mean and standard deviation, most of the geochemical data were studied using the median, first and third quartiles. Those statistics, however, were not used to describe the variability of concentrations of the elements that show either concentrations with bimodal distributions or concentrations below DL in >15% of the samples from certain datasets, (e.g., Au, Ag, As, and Sb in the NMZ and Ag, Sb, and Bi in the MZ). In any of those two situations, the median and quartiles would inadequately represent the element concentrations in the datasets. Therefore, those concentration data were represented by other methods explained in sub-Sections 5.4 and 5.5.

5.4. Geochemical study at deposit-scale

For the deposit-scale geochemical study, the median element concentrations from three datasets were compared. First, element concentrations in the EP were compared with the concentrations in 35 samples from the NMZ. Then, concentrations in the EP were compared with the concentrations in 704 samples from the MZ. Finally, the element concentrations in the MZ were compared with those in the NMZ. The data from the mineralized and non-mineralized zones were extracted from weakly oxidized host rocks in the system of veins and their hanging wall, avoiding samples from MPCs, for testing only the modifications produced in host rocks around the MPCs.

To help in the interpretation of the data, the differences between datasets were represented as percentages of one of the datasets. Differences between the EP concentrations and the median concentrations in the MZ and NMZ were represented as percentage of the EP concentrations. Similarly, differences between median concentrations in the NMZ and median concentrations in the MZ were represented as percentage of the former. The differences between concentrations in the EP and in the NMZ (or MZ) were not calculated if concentrations in the NMZ (or MZ) were below DL and if the DL was higher than the concentration in the EP (calculated with other analytical method). That is because it was uncertain whether the element concentration increased or decreased, depending on how low the actual concentration (expressed as below DL) is. For instance, if the concentrations of Ag are 0.04 ppm in the EP and <0.5 ppm in the NMZ, while the DL is 0.5 ppm, and if the actual Ag concentration in the NMZ is between 0.04 and 0.5 ppm, the Ag concentration would have increased. However, if the actual Ag concentration in the NMZ is below 0.04 ppm, the Ag concentration would have decreased.

If the number of samples with element concentrations below DL was <15% of the total number of samples in a subset of data, the median was used to represent the overall element concentrations in that subset. For the calculation of the median, data below DL were replaced with half of the DL (Carranza, 2011; Reimann and

Filzmoser, 2000). This transformation allowed comparison of median concentrations between datasets.

In contrast, when the number of samples with element concentrations below DL was >15% of the total number of samples in a subset of data, or when the element concentrations showed bimodal distributions, the median was not used. The concentrations of elements showing bimodal distributions in some datasets were represented by the concentrations of the two modes observed in the histograms; then, those two mode concentrations were compared with the median concentrations in other datasets. When >15% of the samples in a subset of data showed concentrations of an element below DL, a median value was calculated by replacing data below DL to the value of the DL; the median element concentration in that subset of data should be lower than the calculated median value. Then, that calculated value was compared with median concentrations from other datasets.

In the NMZ, the distributions of several elements were bimodal. For some of those elements, one of the modes was produced by the concentrations in 12 samples from a lithological unit different from those in the rest of the cross section. This lithological unit is composed of polymictic volcanic breccias, containing thin veinlets of calcite or dolomite and fragments with 1–1.5% disseminated pyrite; it includes abundant black fragments (probably of limestone). These breccias are geochemically different from others in the study area; they show low K_2O, Hg, Be, relatively high Al_2O_3, As, Pb and Cd, and high Na_2O, FeO, CaO, MgO, TiO_2, Cu, Sr, V, Co, Cr, Ni, P and Mn. The source of materials composing those breccias are likely different from the Chon Aike Formation (e.g., Bajo Pobre Formation). The samples from those rocks were omitted from this study, leaving 35 samples in the final dataset. In this final dataset, only Zn, Na_2O and CaO, and the AI and K_2O/Na_2O showed bimodal distributions.

For cross-validating the comparisons of concentrations between the EP and the MZ and NMZ, the "isocon" method of mass balance (Grant, 1986) was applied. The method is derived from the mass balance equations of Gresens (1967), which can be used to calculate gains and losses of elements in altered rocks. Grant (1986) combined volume and density into mass, and derived the equation:

$$C_i^A = M^O/M^A\left(C_i^O + \Delta C_i\right)$$

where C_i^A and C_i^O are the concentrations of element i in the altered rock and the protolith, respectively; M^A is the rock mass of the altered rock, M^O is the rock mass in the protolith and ΔC_i is the change in concentration of element i.

The equation above means that the evaluation of gains and losses of elements depends on the overall rock-mass change of the studied rocks. The rock-mass change can be calculated using elements that were immobile during the alteration, for which $\Delta C_i = 0$. If the values of C_i^O are plotted against values of C_i^A, the immobile elements plot on a straight line that passes through the origin, and has slope M^O/M^A; this line is called an "isocon". The slope of the isocon defines the overall rock-mass change (e.g., slope = 1 if rock-mass change = 0), and is used to calculate mass gains and losses of elements that were mobile during alteration.

Element gains and losses, produced by hydrothermal alteration in the mineralized and non-mineralized zones, were calculated. For that calculation, a rearrangement of the equation above was used (i.e., $\Delta C_i = (M^A/M^O)\ C_i^A - C_i^O$), in which (M^A/M^O) is the inverse of the slope of the isocon.

5.5. Geochemical study at detailed-scale

Data of element concentrations and alteration indices of samples from the MZ and at different distances from the MPCs were plotted in clustered boxplots. Element concentrations in 801 samples from weakly oxidized rocks and in 263 samples from strongly oxidized rocks were used. These samples were extracted from 20 diamond drillcores and only from the system of veins and its hanging wall. For every element and alteration index, data from strongly oxidized and weakly oxidized rocks were represented in separate boxplots for every distance interval from MPCs. The 0 m interval includes samples inside the defined MPCs, while the other intervals include samples outside the MPCs and were defined at every 10 m from the MPCs. In the boxplots, the boxes represent the median, first and third quartiles, while the ends of T-bars represent 1.5 times the inter-quartile range and the values beyond the ends of T-bars are outliers.

The boxplots were used to evaluate (i) the contrast between MPCs and host rocks, (ii) the variations of element concentrations with distance from MPCs, and (iii) the contrast of concentrations between strongly oxidized and weakly oxidized rocks. Curves connecting median concentrations between distance intervals were called "models of compositional variation". Parts of those curves were considered "compositional drifts" when the median concentrations increased or decreased constantly for at least two consecutive intervals. In host-rock dominated materials, the compositional drifts were described by two quantities: "range" and "strength". The range is the distance from the MPCs up to which the compositional drift is preserved. The strength is a measure of the overall slope of the curve that connects median concentrations along a compositional drift.

Most elements with concentrations showing bimodal distributions or with concentrations below DL in >15% of the samples, were not studied with boxplots. In the MZ, data for TiO_2, Sr and Mn exhibit bimodal distributions. The two populations observed for TiO_2 and Sr could not be separated; therefore, these two variables were not represented in the boxplots. In contrast, the two Mn populations were separated; one corresponding to strongly oxidized rocks and the other to weakly oxidized rocks. Because strongly and weakly oxidized rocks are separated in the boxplots, the concentrations of Mn were represented in those plots. Concentrations of Ag, Sb, Bi, Mo, W and Cd were below DL in >15% of the samples; hence, they were not plotted in boxplots.

For Ag, Sb, Bi, Mo, W and Cd, some evaluations were still possible, however. They were carried out to find out the overall differences in element concentrations between the MPCs (interval 0 m) and adjacent host rocks (interval 1–10 m). For this evaluation, we compared the values of two parameters between these two intervals; one of the parameters was the percentage of cases below DL and the other was the median concentration in the interval, calculated with data below DL substituted by the DL.

6. Results and discussion

6.1. Hydrothermal alteration in the study area

The hydrothermal alterations (silicic, argillic and propylitic) in the host rocks often overlap along the studied cross sections (Fig. 5). Pervasive silicification occurs generally in hydrothermal breccias or at <5 m from veins and veinlets; less commonly, it occurs in patches farther away from the veins. Argillic alteration includes clays (illite, kaolinite, scarce smectites and interstratified illite/smectite), which replaced fragments and matrix or were directly deposited in fractures. Propylitic alteration includes mainly chlorite and pyrite; locally it includes calcite, predominant in the deeper parts of the profiles, and very scarce epidote. In the studied cross sections, the spatial link between hydrothermal alterations and veins is only clear for silicification. Most of the rocks affected by silicification are close to veins or veinlets. In cross sections VNS01b and VNS04b (Fig. 5), the pattern of silicification at depth is similar to that of the AC veins. Argillic and propylitic alterations do not show a regular pattern related to the veins; instead they show a slightly different distribution

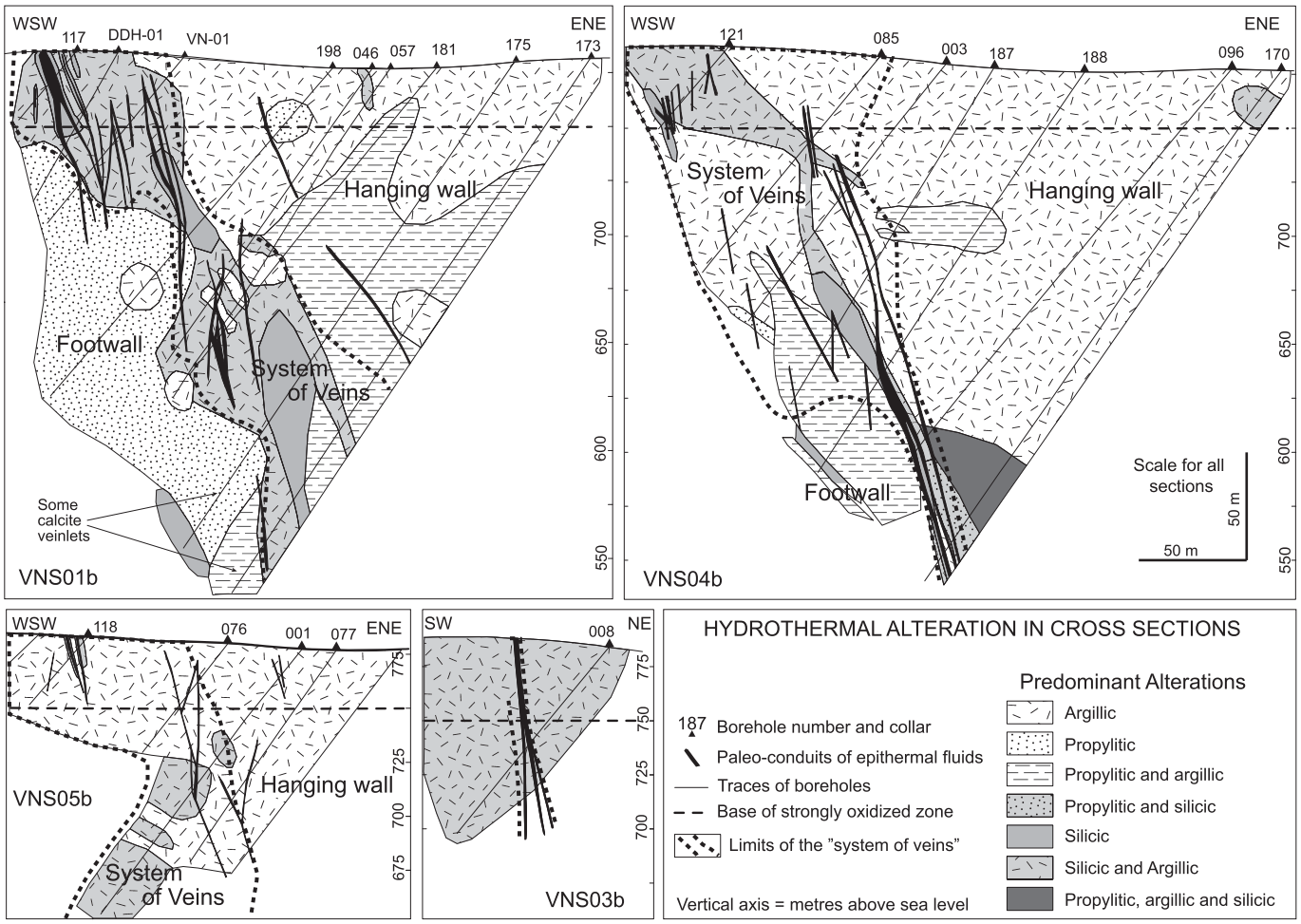

Fig. 5. Hydrothermal alterations in cross sections synthesized from descriptions of drill cores. The system of veins and its footwall and hanging wall are indicated.

related to depth. In general, argillic alteration predominates in the upper part of the profiles, while propylitic alteration predominates in the deeper parts and is absent in the upper parts; both argillic and propylitic alterations are crossed by veins and related silicic alteration (Fig. 5). However, the limited information from the footwall of the Amanda vein, mainly at shallow depth, hinders a more accurate interpretation of the distribution of hydrothermal alterations.

Based on location, predominant hydrothermal alteration and vein mineralogy, three sectors are distinguished in the cross sections of the MZ. The first sector contains the AC veins and surrounding veinlets (Fig. 5), and is referred to here as the "system of veins". This sector includes hydrothermal breccias, abundant veinlets of crystalline quartz with various textures, abundant pyrite and subordinate chalcopyrite, galena, sphalerite, tetrahedrite and bornite. In the system of veins, the distinctive alteration is silicic, which in most cases is overprinted by argillic alteration. The second sector is the "hanging wall" of the system of veins. In this sector, crystalline quartz is almost absent; abundant pyrite and locally chalcopyrite, galena and sphalerite are disseminated and occasionally form veinlets; in the zone of strong oxidation, Fe oxides predominate instead of the sulfides. In the hanging wall, the predominant hydrothermal alteration is argillic, but there is subordinate propylitic alteration; chlorite is locally abundant, mainly at deeper locations, and often related to sulfides surrounding veinlets or disseminated in the groundmass. Veinlets with Au concentrations >0.5 ppm are thin and scarce (in VNS01b and VNS05b). The third sector is the "footwall" of the system of veins, wherein there are scarce veinlets of crystalline quartz and propylitic alteration predominates.

In the NMZ, it is apparent that, despite of limited information, the system of veins, footwall and hanging wall are different in character from those in the MZ. The system of veins, which includes the FEW veins, is composed of only a few crystalline quartz veinlets with some limonite and Mn oxides and with adularia at ground surface. The hanging wall of the FEW veins includes scarce Fe and Mn oxides and very scarce veinlets of chalcedony, and it has no sulfides. The footwall of the veins includes veinlets and disseminations of pyrite and veinlets of calcite. The hydrothermal alteration in the whole profile is a mixture of argillic and silicic alterations. Unlike in the MZ, both argillic and silicic alterations around the FEW veins are weak and argillic alteration only includes illite.

In the MZ, the hydrothermal alterations of the hanging wall extend at least 200 m to the NE of the system of veins. The extent of the alteration halo in the footwall of the veins is undefined because of limited information. However, judging from the extents of the alterations (mainly propylitic) in cross section VNS01b, the footwall at ground surface is altered for more than 100 m to the SW. Therefore, hydrothermal alterations at ground surface cover an area of more than 400 m wide including the system of veins and its walls.

6.2. Timing and relation between mineralization and hydrothermal alterations

The vein fillings and related hydrothermal alterations in the MZ occurred during the initial and main stages of the paragenetic sequence (Fig. 3), while those in the NMZ zone occurred only during the earlier part of the initial stage. The MZ includes the same vein

fillings and hydrothermal alterations observed in the NMZ with the addition of several others previously mentioned for the MZ, including the ore minerals. This suggests that the hydrothermal products in the NMZ represent part of those observed in the MZ. A link between the MZ and NMZ is provided by the correlation of the vein filling in the FEW veins and part of the type (3) vein filling in the AC veins, both containing adularia. The presence of adularia, interpreted as an early mineral, suggests that these two correlated vein fillings are amongst the earliest deposits in the system of veins. In the NMZ, the argillic alterations are devoid of kaolinite, which is common in the MZ. Schalamuk et al. (1998) and Rios et al. (2000) indicated that kaolinite formed only during the main stage of the paragenetic sequence (Fig. 3), and Moreira et al. (2004b) explained that kaolinite might have been derived from alteration of illite or from weathering in a relatively late stage. Therefore, we interpret that the hydrothermal alterations and vein fillings in the NMZ were produced only during the early stages of the veins formation, and that the argillization during these early stages promoted only the formation of illite.

The timing of mineral precipitation in veins and hydrothermal alterations may have been strongly controlled by structural movements during the life of the epithermal system. Dextral movements along curved fractures (Moreira et al., 2008), may have produced local extension in the MZ, promoting the opening of fractures, in contrast to what occurred in the NMZ where the movements along the faults may have produced no extension. In this context, adularia and quartz in the NMZ sealed the original fractures, which remained closed, while in the MZ, the fractures remained open, at least locally, allowing mineral precipitation and formation of several types of vein fillings in the AC veins.

Some relations between Au-mineralization and hydrothermal alterations can be inferred from the spatial relationship between alterations and MPCs. Gold-rich veins and breccias are, up to certain degree, spatially related to silicic alterations; both the high Au concentrations and the silicic alterations are located close to the paleo-conduits. Observed in detail, however, most of the MPCs are partly or completely surrounded by rocks without silicic alteration, but only with argillic or locally propylitic alterations. In addition, silicic alteration alone is often not in contact with the MPCs, although close to them (Fig. 5). These observations suggest that Au-mineralization and silicification occurred during different stages and, probably, under different physico-chemical conditions of the fluids. Therefore, at the paleo-level of the system represented by the study area, silicic alterations can be used as indicators of nearby paleo-conduits but they cannot be used as direct indications of Au-mineralization.

6.3. Geological framework

We consider that the study area represents a portion of a Au–Ag-rich low-sulfidation epithermal paleo-system, located probably in and above the vertical levels of boiling. This portion of the paleo-system includes veins and hydrothermal breccias produced by fluids at temperatures probably <270 °C and mainly composed of crystalline quartz, but also some opal, barite and sulfides, and a limited amount of adularia. Those veins and hydrothermal breccias are hosted mainly by (Upper Jurassic) rhyolitic ignimbrites, which represent the silicic part (post-rift) of a bimodal volcanism, deposited during a generalized extensive event coeval with subduction. In the study area, the hydrothermal alterations around the veins are argillic, silicic and propylitic, in order of abundance. During this study, however, the areas with abundant propylitic alteration were not evaluated.

6.4. Results of the study at deposit-scale

Three assumptions were considered to interpret the results of the study at deposit-scale. The first assumption is that the differences in element concentrations between the EP and the NMZ represent geochemical modifications induced by hydrothermal alterations during a period before mineralization, which is referred to as “alteration phase 1”. The second assumption is that the differences in element concentrations between EP and the MZ represent geochemical modifications induced by hydrothermal alterations before, during and after mineralization. The third assumption is that the differences in element concentrations between the mineralized and non-mineralized zones represent the effects of alterations produced during and after mineralization, a period referred to as “alteration phase 2”.

6.4.1. Comparison between estimated protolith (EP) and the non-mineralized zone

The hydrothermal alterations in the NMZ, which occurred during alteration phase 1, produced minor geochemical changes in the host rocks. The concentrations of Sr, Hg, V, P and Ti in the NMZ are clearly lower than in the EP, but less clearly in the cases of Be, Mo, Al_2O_3, MgO and Mn (Table 1). The concentrations of Ba, Pb and Fe in the NMZ are higher than those in the EP, while those of Co, Cu, Cr and K_2O are similar to those in the EP. The CCPI showed a moderate increase in the NMZ compared to the EP (Table 1).

Although with bimodal distributions, the concentrations of Na_2O are clearly lower in the NMZ than in the EP while that of Zn and the values of AI and K_2O/Na_2O are at least slightly higher in the NMZ than in the EP (Fig. 6; Table 1).

6.4.2. Comparison between estimated protolith (EP) and the mineralized zone

Most geochemical studies of low and intermediate sulfidation epithermal deposits only considered overall effects produced by several alteration stages on lithogeochemistry (e.g., Herrera et al., 1993; Mauk and Simpson, 2007; Warren et al., 2007; Booden et al., 2011). The overall effects of alterations that affected the study area in the La Josefina deposit were inferred by comparing the composition of the EP with that of the MZ.

In the MZ, the hydrothermal alterations produced an overall stronger geochemical change (i.e., predominant enrichment of elements) than in the NMZ. In comparison to the EP, the concentrations of As, Zn, Pb, Co, FeO, Mn, Au, V, Ba, Cu, Cr and Ni are clearly higher in the MZ; those of Na_2O, CaO and Be are notably lower and those of Hg and P are slightly lower. The concentrations of MgO, Al_2O_3 and K_2O in the MZ are similar to those in the EP. Although the concentrations of Sr in the MZ show bimodal distribution, almost all samples from that zone show that the Sr concentrations are lower than in the EP (Fig. 6).

The values of AI and CCPI are higher and K_2O/NaO is much higher in the MZ than in the EP (Table 1). These changes were mainly a function of the leaching of Na and Ca, rather than addition of K. Therefore, the K_2O/Na_2O, as used by other authors to evaluate the intensity of potassium metasomatism in other deposits (e.g., Echavarría et al., 2005; Páez et al., 2010), does not seem to be a reliable indicator of potassium metasomatism in the La Josefina deposit.

The overall concentrations of K_2O in the EP, MZ and NMZ are similar, suggesting that hydrothermal alterations did not add much K to the rocks, even during the stages of deposition of adularia. In addition, the median concentration of K_2O in the study area (around 4%) is close to those reported by other authors (e.g., Warren et al., 2007) for fresh rhyolites and dacites in contrast to higher values reported for K-metasomatized rocks. Even the median concentration of K (ca. 6% K_2O) in the Chon Aike Formation calculated by Peñalva et al. (2005) is higher than the median concentration of K_2O calculated in this study for either the MZ or the NMZ (Table 1).

In other deposits similar to La Josefina, the overall gains and losses of some elements agree with those inferred for the study area (alteration phases 1 + 2), while gains and losses of other elements are substantially different. The behavior of Na, Ca, Sr, Au, As, Ba, Cu, Pb, Zn and Al_2O_3 in the La Josefina deposit, are mostly consistent with

Table 1
Comparison of median element concentrations and alteration indices of three datasets: estimated protolith, mineralized zone and non-mineralized zone.

Elements and indices	DL[a]	Median concentrations			% of values BDL[c]		Percentage of change in concentrations[g]		
		EP[b]	NMZ[d] ($n=35$)	MZ[e] ($n=704$)	NMZ	MZ	From EP to NMZ	From EP to MZ	From NMZ to MZ
Au (ppm)	0.005	0.004	<0.005	0.0190	26	14	nc	375	>280
Ag (ppm)	0.5	0.040	<0.5	<0.6	94	36	nc	nc	nc
Cu (ppm)	1	10	9	15	0	2	−10	50	67
Pb (ppm)	2	20	31	110	0	0	55	448	253
Zn (ppm)	2	40	*80/300*[f]	445	0	0	Increased	1011	Increased
As (ppm)	5	1.5	<10	52	20	2	nc	3367	>420
Sb (ppm)	5	0.2	<5	<5	100	37	nc	nc	nc
Hg (ppm)	0.01	0.08	<0.01	0.06	51	1	<−88	−25.0	>500
Bi (ppm)	2	0.1	<2	<3	97	34	nc	nc	nc
Mo (ppm)	1	2	<1	<2	100	23	<−50	<0	nc
W (ppm)	10	2	<10	<10	100	44	nc	nc	nc
Ba (ppm)	10	600	1170	890	0	0	95.0	48.0	−24.0
Be (ppm)	0.5	5.0	2.8	1.5	0	2	−44	−70	−46
Sr (ppm)	1	285	63	*19/80*	0	0	−78.0	Decreased	nc
V (ppm)	1	20	5	44	0	0	−75	120	780
Cr (ppm)	1	4	3	7	0	3	−25	75	133
Ni (ppm)	1	0.5	<1	3	26	12	nc	500	>200
Cd (ppm)	0.5	0.2	<0.5	<1.2	86	34	nc	nc	nc
Co (ppm)	1	1	1	8	14	1	0	700	700
P (ppm)	10	175	80	120	0	0	−54.0	−31.0	50.0
Mn (ppm)	5	387	318	1065.0	0	0	−18.0	175.0	235.0
Al_2O_3 (%)	0.0189	14.565	12.977	13.119	0	0	−10.9	−9.9	1.1
K_2O (%)	0.0121	4.360	4.145	4.410	0	0	−5	1.2	6.4
Na_2O (%)	0.0135	2.990	*0.08/1.30*	0.094	0	1	Decreased	−97.0	nc
CaO (%)	0.014	1.675	*0.09/1.20*	0.056	0	0	Decreased	−97.0	Decreased
MgO (%)	0.0166	0.400	0.282	0.365	0	0	−29.5	−8.8	29.3
FeO (%)	0.0129	1.480	1.775	5.369	0	0	20.0	263.0	202.0
TiO_2 (%)	0.0167	0.165	0.067	*0.06/0.35*	0	1	−59.0	nc	nc
Al		49.26	*64/96*	96.70			nc	91.00	nc
CCPI		19.97	29.15	55.27			46.00	171.00	90.00
K_2O/Na_2O		1.49	*4.2/57*	46.34			nc	3078.00	684.00

[a] DL = detection limit of the analytical methods.
[b] EP = estimated protolith. Concentration of P, Mn, Al_2O, K_2O, CaO, MgO, FeO andTiO_2 in EP, were calculated with 28 samples from Alperin Et al. (2007); for other elements they are average abundances in granites (Levinson, 1974).
[c] BDL = below DL.
[d] NMZ = Non-mineralized zone.
[e] MZ = Mineralized zone. Symbol "<" indicates that more than 15% of the samples yielded concentrations BDL.
[f] In bimodal distributions, aproximate concentrations of both modes are indicated in italic characters.
[g] Negative percentages of chage indicate depletion; positive indicate enrichment. When concentrations in the NMZ (or MZ) are BDL, and the DL is higher than the concentration in the EP, percentages of change between the EP and the NMZ (or MZ) were not calculated ("nc"), because there may have been either a gain or a loss, depending on the actual concentration (expressed as below DL). When one of the datasets showed bimodal distribution of an element concentration, percentages of change were not calculated because a median concentration for that element was not available. If both modes in the bimodal distribution showed a different result (gain/loss) we displayed "nc"; if both modes showed the same result, we indicated it as "Decreased" or "Increased".

those described in the literature. General depletions in Na, Ca and Sr agree with the results of several studies (Gemmell, 2007; Mauk and Simpson, 2007; Murakami and Feebrey, 2001; Silberman and Berger, 1985). Gains of Au and As were observed in the Round Mountain, Harsbrouk Mountain, Gosowong, Golden Cross, Yamagano and Axi deposits, and in some deposits in the northern Great Basin of the United States (Berger and Silberman, 1985; Gemmell, 2007; John, 2001; Mauk and Simpson, 2007; Murakami and Feebrey, 2001; Zhai et al., 2009), while gains of Ba were registered by Darce et al. (1991) and Booden et al. (2011); although Ba concentrations are considered to have increased particularly in intermediate sulfidation deposits (John, 2001). As in the La Josefina, gains of Cu, Pb and Zn were observed in the Gosowong deposit (Gemmell, 2007) and some deposits in the Great Basin (John, 2001); but, losses of these elements were reported in the Axi deposit (Zhai et al., 2009). Several authors considered Al_2O_3 as immobile or weakly mobile (Booden et al., 2011; Darce et al., 1991; Mauk and Simpson, 2007; Silberman and Berger, 1985); this is also apparently the case in the La Josefina deposit.

The behaviors of MgO, FeO, Co, Ni and K_2O in the La Josefina deposit are different from those described in the literature. Unlike in La Josefina where MgO is rather immobile, MgO is quite mobile in other deposits (Booden et al., 2011; Gemmell, 2007; Silberman and Berger, 1985). Iron was gained in the La Josefina deposit, it was lost in the Waitekauri Area (Booden et al., 2011), locally lost in the Golden Cross deposit (Mauk and Simpson, 2007), and slight mobile in the La Libertad deposit (Darce et al., 1991). Cobalt and Ni were gained in the La Josefina deposit, but were immobile in the Golden Cross deposit (Mauk and Simpson, 2007). Potassium, which exhibits weak mobility in the study area, exhibits gains in altered rocks around many other deposits of this type (Booden et al., 2011; Darce et al., 1991; Gemmell, 2007; Mauk and Simpson, 2007; Murakami and Feebrey, 2001; Silberman and Berger, 1985).

Differences amongst deposits show the geochemical variability amongst them (Hedenquist et al., 2000; Silberman and Berger, 1985). The geochemical variability may be attributed to genetic differences amongst deposits, differences that eventually may deserve a more detailed deposit classification. However, geochemical variability amongst deposits may also be attributed to different compositions of the protolith, and different types of alteration. Gains of K_2O, for instance, are not so noticeable when the protolith is a rhyolitic rock because of the relatively high initial K_2O content (in K-feldspars); in addition, the gains may be higher in adularia-rich rocks than in illite and illite/smectite-rich rocks, as was observed by Booden et al. (2011). In the study area of the La Josefina deposit, the rhyolitic protolith and the hydrothermal alterations with predominant illite and

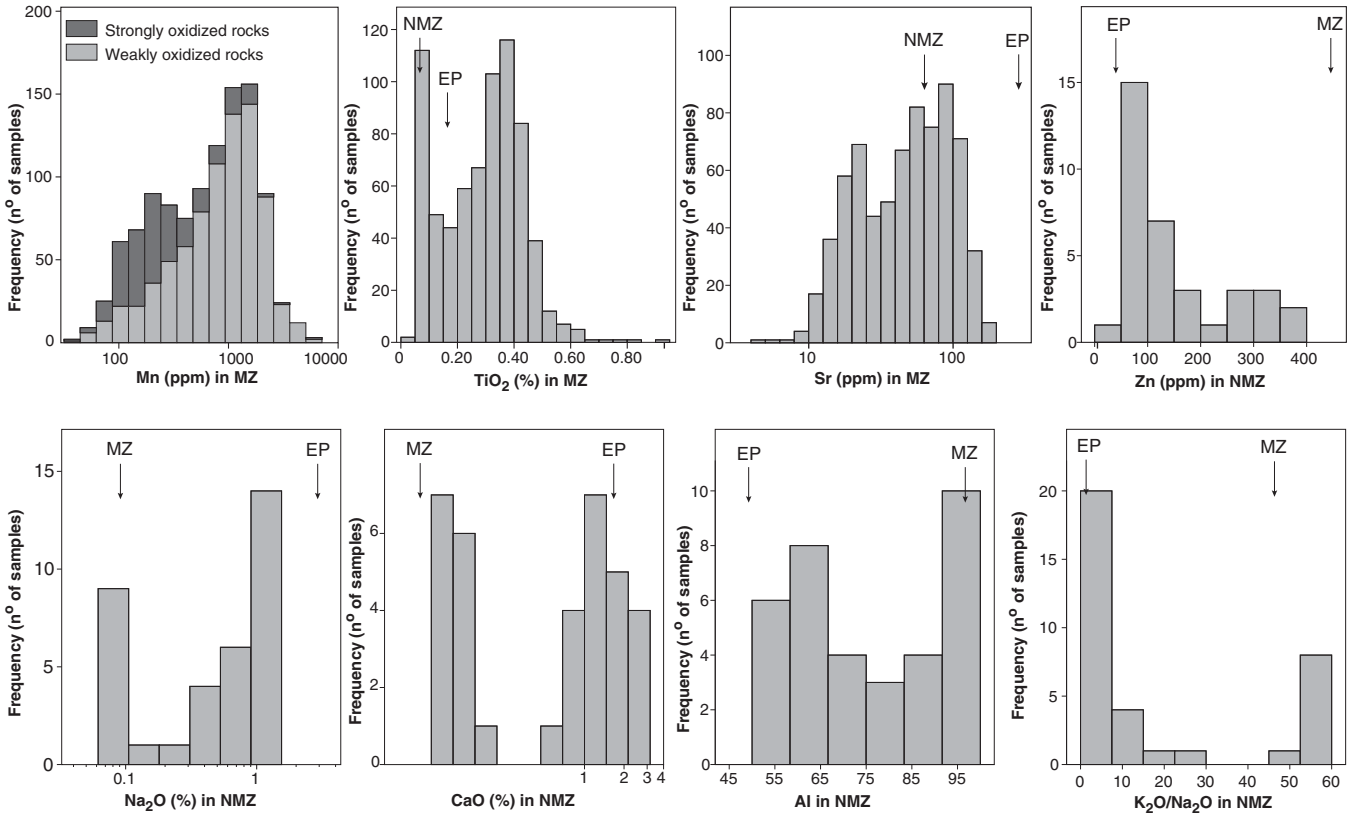

Fig. 6. Histograms showing bimodal distributions of Mn, TiO_2 and Sr in the mineralized zone (MZ), and of Zn, Na_2O, CaO, Al and K_2O/Na_2O in the non-mineralized zone (NMZ). EP = estimated protolith. Arrows indicate median concentrations in the other datasets.

abundant chlorite probably explain why K_2O exhibits only weak mobility. Because most studied deposits are hosted by andesitic or dacitic rocks, the results from those studies are probably not directly comparable to the La Josefina and similar deposits hosted in rhyolitic rocks (e.g., Round Mountain and Harsbrouk Mountain).

6.4.3. Isocon method of mass balance

In the application of the isocon method, aluminum was selected as immobile element. This was the most reasonable choice because aluminum is relatively immobile in hydrothermal deposits (Booden et al., 2011; Darce et al., 1991; Mauk and Simpson, 2007; Silberman and Berger, 1985), and other potential immobile elements, such as Zr, Th and some REEs are not available in the dataset, while TiO_2 showed a bimodal distribution. The isocon, which has a slope of 0.89 (Fig. 7), was traced using only the median concentration of Al_2O_3 from the NMZ. According to the slope of the isocon, and in comparison to the EP, the overall rock-mass increased by about 12% due to alteration. This is likely due to the addition of sulfides and silica into the host rocks, which probably occupied original pores of the rock.

The results of applying the isocon method to the datasets (Fig. 7) show that in the NMZ, Cu, Mn, K_2O, Co and Al_2O_3 are close to (or on) the isocon, while in the MZ, Al_2O_3, MgO and K_2O are close to the isocon. Because Al_2O_3 and K_2O are close to the isocon in both zones, we interpret that they were relatively immobile or that, in general, the host rocks did not gain or lost considerable amounts of those substances during interaction with the hydrothermal fluids.

In general terms and considering some margin of error, the differences in element concentrations obtained by comparing the concentrations in the EP with those in the MZ and NMZ are coincident with the results produced by the mass balance using the isocon method (Fig. 7). Therefore, the general tendencies obtained from the comparisons without using mass balance analysis are considered reliable, and can be used to draw conclusions about the effects of hydrothermal alterations on the geochemistry. However, the amount of overall rock-mass increase gives an idea of the possible error that should be considered when using the geochemical data without mass balance analysis.

6.4.4. Comparison between the mineralized and non-mineralized zones

The median concentrations of As, V, Co, Mn, FeO, Au, Pb, Cu, Hg, Cr, Ni, P and MgO in the MZ are higher than in the NMZ, while those of Ba and Be are lower, and those of Al_2O_3 and K_2O are similar. Despite showing bimodal distributions in the NMZ, the concentrations of Zn in the MZ are clearly higher than in the NMZ, while those of CaO are clearly lower (Fig. 6; Table 1). In contrast, concentrations of Sb, Bi, Mo, W and Cd in the MZ could not be compared with those in the NMZ because they are below DL in >15% of the samples from both zones. Concentrations of Sr, Na_2O and TiO_2, and values of Al and K_2O/Na_2O could not be compared because they show bimodal distributions in one of the datasets, and the modes in the histogram from that dataset are not clearly different from the median of the other dataset (Fig. 6).

6.5. Result of the study at detailed-scale

Detailed-scale variations in element concentrations with distance to mineralized veins, are not well documented for low and intermediate sulfidation deposits. In the Bodie Bluff district, Silberman and Berger (1985) investigated variations in concentrations of Au, K, Sr, Ag, Zn, As, Hg, Sb, Mn and Cu with distance from three mineralized veins, but only up to 7.5 m from the veins, using a limited number of samples, and considering, along the investigated distance interval, concentrations of individual samples. For most investigated elements,

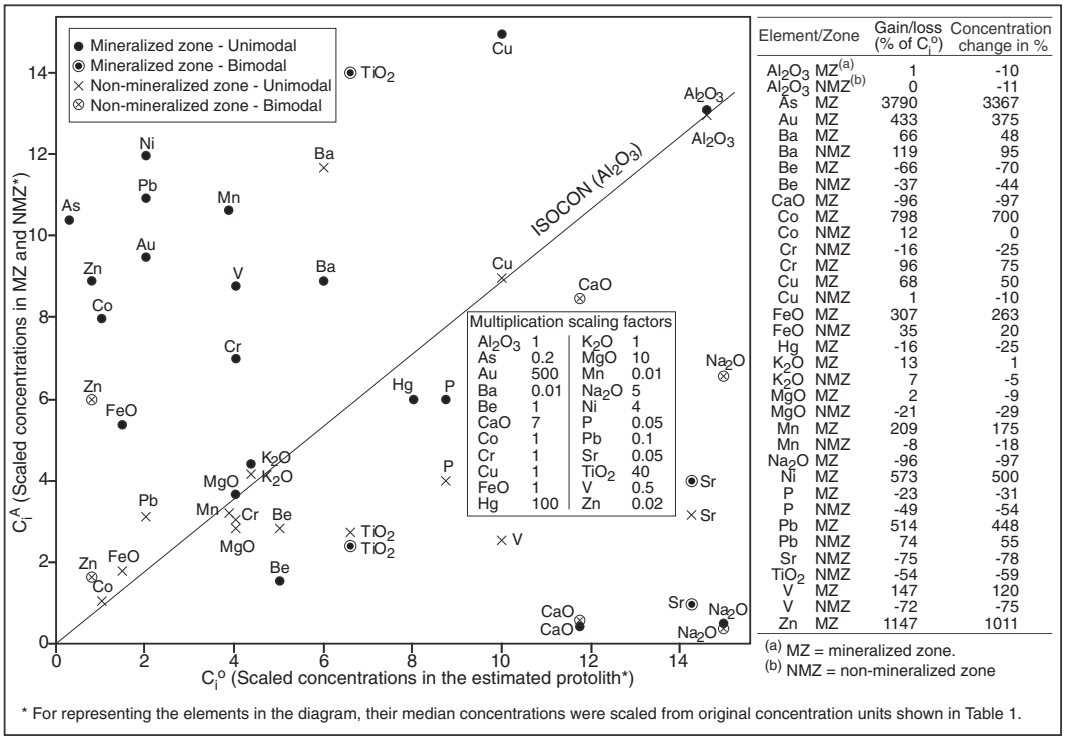

Element/Zone		Gain/loss (% of C_i^o)	Concentration change in %
Al_2O_3	MZ[a]	1	-10
Al_2O_3	NMZ[b]	0	-11
As	MZ	3790	3367
Au	MZ	433	375
Ba	MZ	66	48
Ba	NMZ	119	95
Be	MZ	-66	-70
Be	NMZ	-37	-44
CaO	MZ	-96	-97
Co	MZ	798	700
Co	NMZ	12	0
Cr	NMZ	-16	-25
Cr	MZ	96	75
Cu	MZ	68	50
Cu	NMZ	1	-10
FeO	MZ	307	263
FeO	NMZ	35	20
Hg	MZ	-16	-25
K_2O	MZ	13	1
K_2O	NMZ	7	-5
MgO	MZ	2	-9
MgO	NMZ	-21	-29
Mn	MZ	209	175
Mn	NMZ	-8	-18
Na_2O	MZ	-96	-97
Ni	MZ	573	500
P	MZ	-23	-31
P	NMZ	-49	-54
Pb	MZ	514	448
Pb	NMZ	74	55
Sr	NMZ	-75	-78
TiO_2	NMZ	-54	-59
V	MZ	147	120
V	NMZ	-72	-75
Zn	MZ	1147	1011

[a] MZ = mineralized zone.
[b] NMZ = non-mineralized zone

Fig. 7. Isocon diagram and table based on median concentrations for the mineralized and non-mineralized zones. The isocon line (slope = 0.89) is based on the concentrations of aluminum as immobile element. The median concentrations of elements were scaled to represent them in the same diagram. The table shows a comparison between the gains and losses of elements calculated with the isocon method of mass balance and the change in concentration calculated without mass balance (from Table 1); both are represented in percentages of the concentrations in the estimated protolith (C_i^O). Zinc, Sr, Na_2O, CaO and TiO_2 show bimodal distributions in one of the zones; thus, the approximate values of both modes were plotted with distinct symbols but were not shown in the table. Elements that show concentrations below DL in >15% of the samples from one or both zones are not shown in the figure.

this approach produced strongly irregular variations, which cannot be used to indicate proximity to mineralized veins. In contrast, we plotted element concentrations as median values of several samples within distance intervals from MPCs, showing a more continuous and consistent variation with distance from veins.

Along the studied intervals from MPCs, the boxplots and models of compositional variation clearly represent the continuous compositional variations of the rocks. For most of the elements, these models show increasing or decreasing compositional drifts along a few distance intervals (Fig. 8; Table 2), but the boxplots show strong overlap between adjacent distance intervals. This shows the strong dispersion of element concentrations in every interval, which produces relatively large interquartile ranges.

The behaviour of the elements during the formation of MPCs can be inferred from the geochemical contrast between the 0 m interval, which represents materials deposited from the hydrothermal fluids, and the 1–10 m interval, which represents the host rocks. Relative to their adjacent host rocks, the MPCs (0 m interval) show much higher concentrations of Au, Cu, As, Hg, Pb and Co, much lower concentrations of Al_2O_3, K_2O, Na_2O, CaO, MgO and Ba, and slightly lower concentrations of Mn and P. Despite the high number of samples with element concentrations below DL, the concentrations of Ag, Sb, and Bi are clearly higher in the MPCs, where they show a low percentage of samples with element concentrations below DL (Table 3). The concentrations of Mo and Cr seem to be similar in the MPCs and its immediate host rocks, while those of Cd and W seem to be higher in the MPCs, although they are difficult to evaluate because of their small differences and the high number of undetermined values (Table 3). In addition, Ag, Cu, Pb, As, Sb, Bi and Cd are associated with Au in native gold, electrum, pyrite, chalcopyrite and galena. These observations suggest that the processes that formed the mineralized veins and hydrothermal breccias were accompanied by precipitation of Au, Ag, Cu, As, Hg, Pb, Co, Sb and Bi, and probably Cd and W.

The studied elements generally show either enrichment or depletion relative to the EP along the entire 60 m interval from the MPCs. For some elements, however, both enrichment and depletion occur at different distances from the MPCs; K_2O, MgO, Cu, Hg, Ba and P (Fig. 8) show both enrichment and depletion in different parts of that interval. This is important because geochemical data in the proximity of a MPC may indicate either depletion or enrichment, depending on the distance from the MPC. The variations of element concentrations beyond the MPCs represent compositional changes produced by hydrothermal alterations in the host rocks, and are more subtle than the changes that include the MPCs. The strongest overall compositional drifts in host-rock dominated materials are those of P, Au, Cu, Pb, Hg, Ba and MgO, which reach up to 40 m from the MPCs, except for Au (Table 4; Fig. 8). Concentrations of Mn, As, FeO, K_2O, Na_2O, Al_2O_3 and Ni show weaker compositional drifts. Calcium, Co, Be, V and Zn show no clear compositional drifts in the host rock.

6.6. Geochemical indicators

At deposit-scale, comparison of the MZ with the NMZ, which are both hydrothermally altered, shows that the concentrations of As, V, Co, Mn, FeO, Au, Pb, Cu, Hg, Cr, Ni, P, MgO and Zn (and values of CCPI) are higher in the MZ than in the NMZ, while those of Ba, Be and CaO are lower in the MZ than in the NMZ. These 18 variables are therefore, geochemical indicators of the mineralized altered zone.

At detailed-scale, P, Au, Cu, Pb, Hg, Ba and MgO display the strongest compositional drifts, and thus are the best geochemical indicators

of proximity to mineralized rocks. Manganese, As, FeO, K_2O, Na_2O, Al_2O_3 and Ni show weaker compositional drifts; therefore, they are poor indicators of proximity to mineralized rocks.

6.7. Effects of weathering

Weathering has affected the concentrations of Cu, Na_2O, MgO, FeO, As, Pb, Co, Ba, Mn and Zn. The most affected elements were Cu, Pb, Co, Mn, MgO and Zn. The concentrations of these elements in weakly oxidized and strongly oxidized rocks are clearly different (Fig. 8). The median concentration of Cu in the strongly oxidized samples of the MPCs (654 ppm) is notably lower than in the weakly oxidized samples (2620 ppm). In the host rocks, the opposite occurs (Table 2; Fig. 8b). This suggests that some Cu in the MPCs became mobile and was re-deposited at a distance. In strongly oxidized rocks, the median concentrations of MgO, Co, Mn and Zn are lower than in the weakly oxidized rocks along the whole 60 m interval. In contrast, concentrations of Pb in the strongly oxidized rocks are higher along the whole interval (Fig. 8c). The concentrations of Na_2O, Ba, As and FeO were slightly affected by weathering; those of Na_2O and Ba show the effects of weathering only in the MPCs, while those of As show the effects of weathering only far away from the MPCs. The other studied elements were not considerably affected by weathering.

Near the surface where weathering is stronger, the usefulness of several elements as geochemical indicators of mineralized rocks is a function of the scale of study. From a deposit-scale perspective, weathering did not modify considerably the usefulness of the geochemical indicators of mineralized zones because increases in their concentrations at certain distances from MPCs were compensated

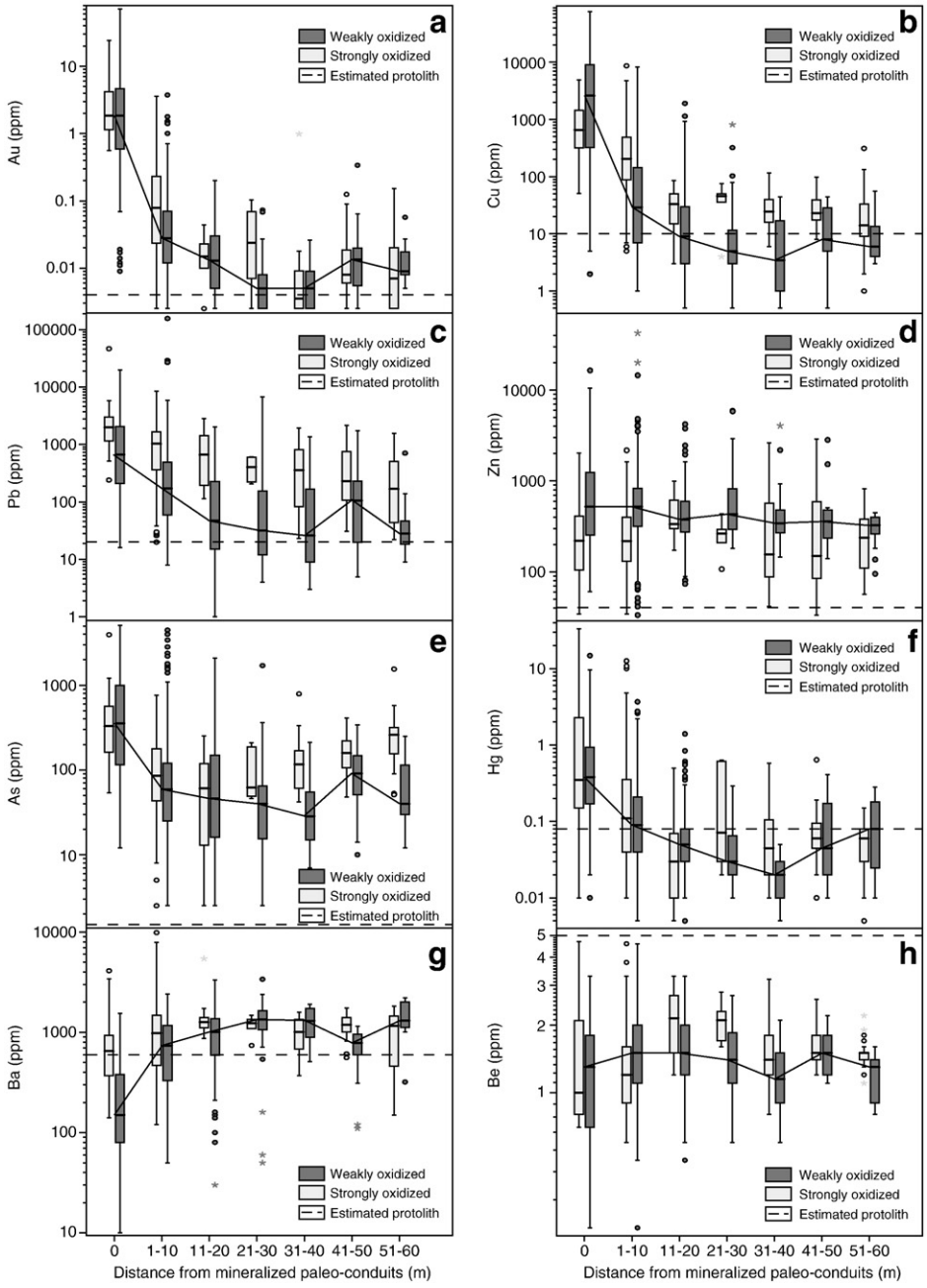

Fig. 8. Boxplots and models of compositional variation with data from the mineralized zone. Distance 0 coincides with the mineralized paleo-conduits. Small circles are regular outliers; asterisks are extreme outliers.

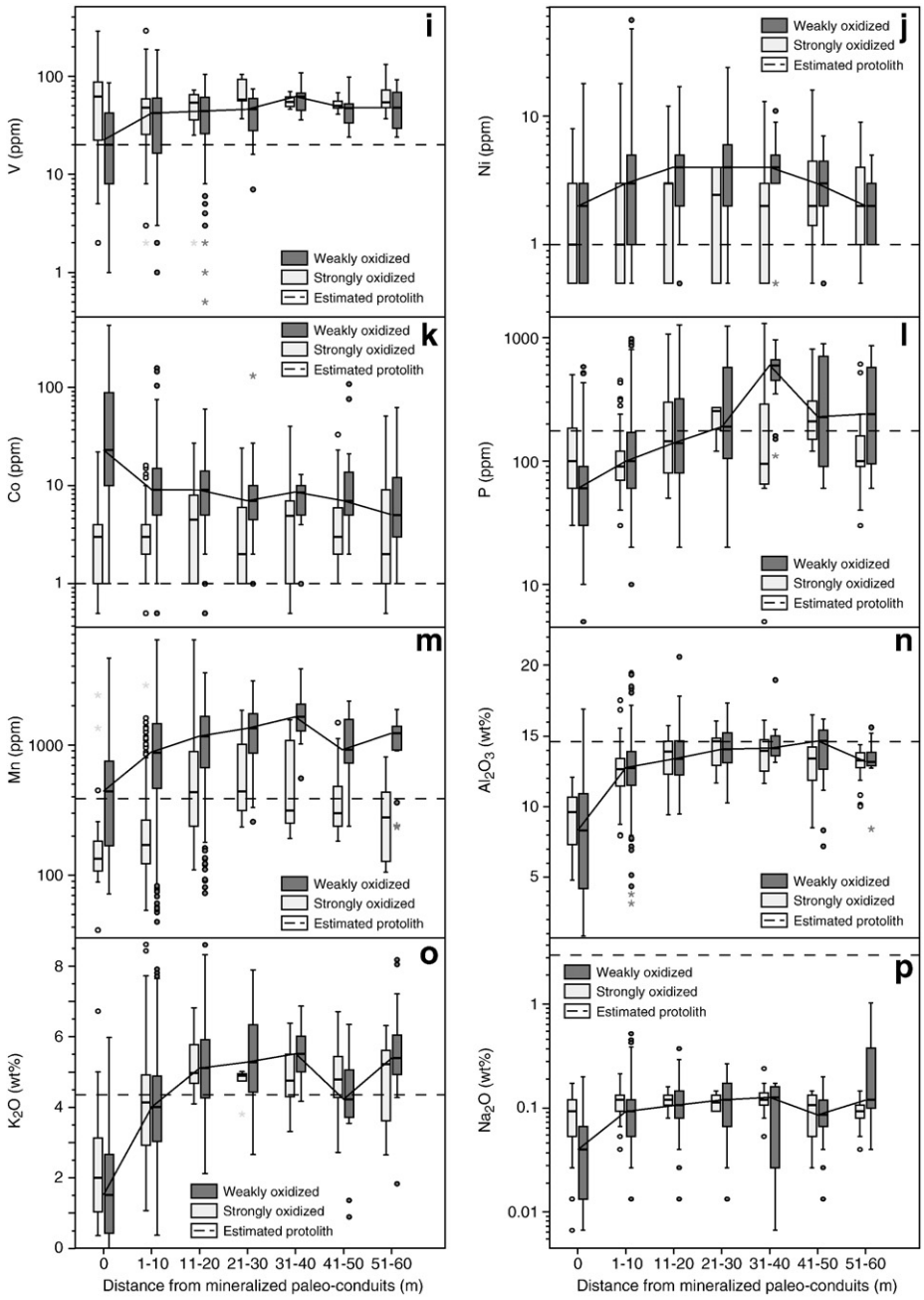

Fig. 8 (*continued*).

with decreases in their concentrations at other distances. Most elements show similar overall median concentrations in the strongly oxidized and in the weakly oxidized rocks, and thus they can be used as geochemical indicators of mineralized zones at deposit-scale. From a detailed-scale perspective, in contrast, weathering decreased the usefulness of several elements as geochemical indicators of proximity to MPCs. Compositional drifts defined by the concentrations of Pb, Na_2O, FeO and Ba, and the values of CCPI in the weakly oxidized rocks disappear or become irregular and weaker in the strongly oxidized rocks (Table 4). Therefore, these geochemical variables are unsuitable indicators of proximity to MPCs in weathered rocks.

Other authors have studied the effects of weathering on the concentrations of Ca, Na, K, Fe, Mg and aluminum in rocks that are similar to those in La Josefina, although in areas not related to mineral deposits. In most cases, their results do not agree with ours, except those showing strong leaching of Mg (Guan et al., 2001; Selby, 1993), which also occurred by weathering in the La Josefina deposit. In contrast to our results, which show that Fe and aluminum were almost not modified by weathering, Malpas et al. (2001) found that the concentrations of these elements were increased by weathering. In the La Josefina and other areas related to similar mineral deposits it is plausible that concentrations of FeO were not increased by weathering because of the likely oxidation and subsequent partial leaching of relatively abundant Fe-sulfides, introduced into the host rocks by previous hydrothermal alteration; although part of the iron is fixated in Fe-oxides. Regarding aluminum, we consider it as nearly immobile during hydrothermal alteration and weathering in the La Josefina and likely in areas with similar conditions, although it is possible that minor amounts of aluminum were moved locally by eluvial processes from the surface to lower soil horizons (Chittleborough, 1991).

Calcium, Na and K were invariably leached by weathering in other areas (Chan et al., 2007; Guan et al., 2001; Malpas et al., 2001; Selby,

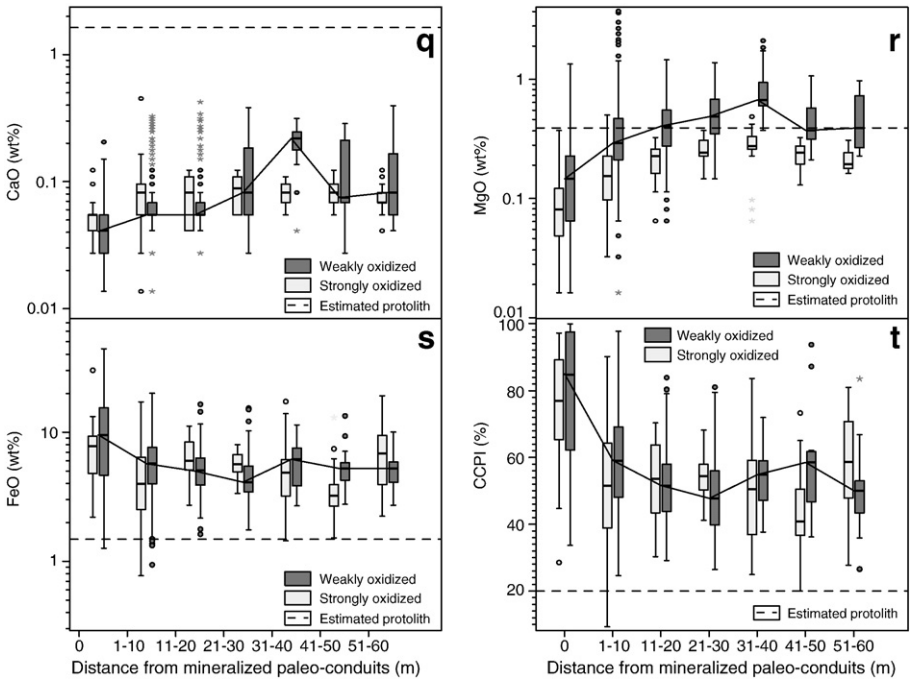

Fig. 8 (*continued*).

1993), while in the La Josefina area, those elements were mostly unaffected by weathering. In the study area, weathering likely had no opportunity to leach Ca and Na considerably because the concentrations of these elements were already low due to previous hydrothermal alterations. The limited modification of K concentrations in the La Josefina area in contrast to other studied areas may have also been due to the previous hydrothermal alterations. These alterations probably transferred some K from K-feldspars of the original host rocks to other K-rich minerals, predominantly illite, which are not strongly affected by weathering; this resulted in the overall near immobility of K during hydrothermal alteration, as well as weathering.

6.8. Implications for exploration

In the La Josefina epithermal system, hydrothermally altered zones that were mineralized with Au likely show different alteration mineralogy compared to those that were not mineralized. Alterations prior to Au-mineralization (alteration phase 1) included weak silicification and argillization of the host rocks around the veins. Those argillic alterations are mainly composed of illite, while kaolinite is absent. Alterations resulting from the complete hydrothermal process (alteration phases 1 and 2), including the stages of Au-mineralization, are silicic and argillic, partially overprinted by propylitic. In contrast to alterations during phase 1, the alterations during phase 2 seem to have been stronger and included abundant kaolinite as one of the predominant minerals.

In addition to considering the overall effects on lithogeochemistry by all alterations that affected the study area, which only shows net gains and losses (i.e., difference between the initial and final conditions), we attempted to isolate the geochemical modifications of the host rocks produced during the events of mineralization. This was done by inferring the changes produced during the two consecutive alteration phases, 1 and 2, and by integrating data from the detailed-scale part of the study and from previous mineralogical studies. Although that isolation cannot be completely accomplished, because the alterations contemporaneous with mineralization are overprinted by others, we prefer our approach of considering different phases of alteration, rather than the overall effects of all alteration events. This approach gives more flexibility to extrapolate the results to other areas of the deposit or to similar deposits, under slightly different conditions to those in the study area.

Elements that were lost or gained during alteration phase 1 in contrast to alteration phase 2, can be used to effectively distinguish potentially mineralized zones from barren zones. Alteration phase 1 resulted in losses or no modifications for Au, Cu, Hg, V, Co, Mn, MgO, Cr and P, while alteration phase 2 resulted in gains of those elements. The concentrations of Ba increased during alteration phase 1 but decreased during alteration phase 2. In addition, other elements experience either loss or gain during both alteration phases; while concentrations of Pb, Zn and FeO, (and values of CCPI) increased, and those of Be and CaO decreased. Although it was not possible to assess the effects of alteration phase 1 on As and Ni because of the high number of samples with concentrations below DL, the concentrations of these two elements are higher in the MZ than in the NMZ. Therefore, all these 18 geochemical variables are useful geochemical indicators to differentiate between mineralized and non-mineralized zones, but Au, Cu, Hg, V, Co, Mn, MgO, Cr, Ba and P are probably the most effective.

These 18 geochemical variables can be used to distinguish between mineralized and non-mineralized zones in other parts of the deposit, if the sampling procedure and the general geological conditions are similar to those of the study area. The sampling procedure should avoid samples from MPCs and should represent different distances from them. This can be achieved by sampling areas of at least a few tens of metres wide and omitting samples that show values of Au higher than 0.5 ppm. The geological conditions that must be satisfied include the approximate position in the paleo-system; this is difficult to know at the beginning of exploration but, at least, indicators of proximity to paleo-surface such as sinters, blankets of abundant kaolinite or extended pervasive silicification should be absent. The geological conditions should also include relatively homogeneous lithologies of rhyolitic to rhyodacitic compositions, and the absence of abundant propylitic alteration.

In slightly different geological conditions, however, a few elements may be useful indicators of mineralized zones. Some elements

Table 2
Statistics for element concentrations in distance intervals from mineralized paleo-conduits, using separate datasets for strongly oxidized and weakly oxidized rocks.

		Distance intervals in weakly oxidized rocks (m)							Distance intervals in strongly oxidized rocks (m)						
		0	1–10	11–20	21–30	31–40	41–50	51–60	0	1–10	11–20	21–30	31–40	41–50	51–60
Element	Statistics[a]	n 97	435	161	55	22	16	15	27	140	14	6	20	23	33
Au (ppm)	Q1	0.579	0.012	0.005	0.003	0.003	0.005	0.008	1.150	0.023	0.008	0.006	0.003	0.006	0.003
	Median	1.845	0.028	0.013	0.005	0.005	0.014	0.009	1.860	0.079	0.015	0.036	0.004	0.008	0.007
	Q3	4.780	0.070	0.031	0.008	0.009	0.021	0.019	4.260	0.231	0.023	0.078	0.011	0.019	0.023
Cu (ppm)	Q1	311	7	3	3	1	5	4	295	88	13	28	15	17	9
	Median	2620	29	9	5	4	8	6	654	206	33	46	25	23	14
	Q3	10150	143	31	12	17	29	15	1520	489	55	57	41	40	34
Pb (ppm)	Q1	205	59	15	12	9	19	18	1070	352	180	220	82	78	38
	Median	667	171	47	32	27	107	28	1990	1030	665	417	360	231	169
	Q3	2150	506	228	157	195	321	63	3040	1665	1570	600	820	857	512
Zn (ppm)	Q1	250.5	313	270.5	291	258.3	216.3	254	99	129.3	270.3	181.8	86.5	79	107
	Median	514	515	374	426	339	354	321	217	215.5	331.5	261.5	154	148	234
	Q3	1230	820	593	808	474.8	487.8	409	422	395.5	618	324.3	581	632	385
As (ppm)	Q1	111	25	16	15	15	50	27	149	43	13	48	58	99	149
	Median	356	59	46	40	29	92	40	330	86	62	63	117	159	260
	Q3	1005	120	155	67	55	164	194	589	180	122	194	171	225	336
Hg (ppm)	Q1	0.155	0.040	0.030	0.020	0.010	0.020	0.020	0.140	0.040	0.010	0.028	0.020	0.040	0.030
	Median	0.380	0.090	0.050	0.030	0.020	0.045	0.080	0.350	0.110	0.030	0.100	0.045	0.060	0.060
	Q3	0.970	0.210	0.080	0.070	0.030	0.193	0.190	2.340	0.363	0.075	0.615	0.108	0.100	0.080
Ba (ppm)	Q1	80	330	585	1050	878	558	1110	360	460	1100	1003	670	980	440
	Median	150	740	1010	1340	1305	785	1310	650	980	1265	1230	1010	1190	1160
	Q3	390	1180	1375	1660	1745	958	2150	960	1493	1440	1375	1380	1430	1470
Be (ppm)	Q1	0.7	1.1	1.2	1.1	0.9	1.2	0.9	0.8	0.9	1.5	1.7	1.2	1.4	1.4
	Median	1.3	1.5	1.5	1.4	1.2	1.5	1.3	1.0	1.2	2.2	2.1	1.4	1.5	1.5
	Q3	1.8	2.0	2.0	1.9	1.5	1.9	1.4	2.3	1.6	2.8	2.4	1.8	1.8	1.6
V (ppm)	Q1	8	16	26	28	45	33.25	28	107	122	234	295	247.5	230	127
	Median	20	42	44	46	62	47.5	48	134	171.5	440.5	447.5	313.5	300	279
	Q3	42	60	61.5	60	67	53.25	70	189	267.5	906.5	1220	1245	653	439.5
Ni (ppm)	Q1	0.5	1.0	2.0	2.0	3.0	2.0	1.0	0.5	0.5	0.5	0.5	0.5	1.0	1.0
	Median	2.0	3.0	4.0	4.0	4.0	3.0	2.0	1.0	1.0	3.0	2.5	2.0	2.0	2.0
	Q3	3.0	5.0	5.0	6.0	5.0	4.8	3.0	3.0	3.0	3.3	4.0	3.0	5.0	5.0
Co (ppm)	Q1	10	5	5	4	5	5	3	1.0	2.0	1.0	1.0	1.0	2.0	1.0
	Median	23	9	9	7	9	7	5	3.0	3.0	4.5	2.0	5.0	3.0	2.0
	Q3	89	15	14	10	10	16	12	4.0	4.0	8.5	10.5	7.0	7.0	10.0
P (ppm)	Q1	30	60	80	100	433	90	90	60	70	78	165	63	150	90
	Median	60	100	140	190	595	230	240	100	90	150	255	95	210	100
	Q3	95	170	325	580	673	713	640	190	120	360	270	300	310	170
Mn (ppm)	Q1	168	457	671	848	1275	718	901	107	122	234	295	248	230	127
	Median	442	875	1170	1345	1645	921	1230	134	172	441	448	314	300	279
	Q3	753	1460	1663	1750	2155	1660	1400	189	268	907	1220	1245	653	440
Al_2O_3 (%)	Q1	4.08	11.52	12.26	13.07	13.59	12.48	12.88	6.99	11.47	12.11	12.63	12.52	11.49	12.71
	Median	8.33	12.75	13.39	14.07	14.16	14.66	13.17	9.62	12.66	13.92	14.64	13.95	13.41	13.30
	Q3	10.94	13.92	14.66	15.30	15.03	15.43	13.94	10.69	13.43	14.73	15.17	14.81	14.30	13.84
K_2O (%)	Q1	0.42	3.04	4.27	4.41	4.99	3.68	4.92	0.90	2.92	4.68	4.51	4.27	4.28	3.59
	Median	1.52	4.01	5.11	5.28	5.52	4.23	5.40	2.00	4.13	4.97	4.90	4.76	4.78	5.22
	Q3	2.73	4.89	5.92	6.36	6.02	5.06	6.29	3.17	4.92	5.90	4.97	5.53	5.80	5.65
Na_2O (%)	Q1	0.01	0.05	0.08	0.07	0.03	0.07	0.09	0.05	0.09	0.11	0.09	0.11	0.05	0.07
	Median	0.04	0.09	0.11	0.12	0.13	0.09	0.12	0.09	0.12	0.12	0.11	0.12	0.11	0.09
	Q3	0.07	0.12	0.15	0.18	0.16	0.13	0.84	0.12	0.13	0.13	0.14	0.14	0.13	0.11
CaO (%)	Q1	0.03	0.06	0.06	0.06	0.17	0.07	0.06	0.04	0.06	0.04	0.06	0.07	0.07	0.06
	Median	0.04	0.06	0.06	0.08	0.22	0.08	0.08	0.06	0.08	0.08	0.09	0.08	0.08	0.07
	Q3	0.06	0.07	0.07	0.20	0.25	0.22	0.29	0.06	0.10	0.12	0.12	0.10	0.10	0.09
MgO (%)	Q1	0.07	0.22	0.27	0.35	0.59	0.31	0.25	0.05	0.10	0.16	0.21	0.27	0.20	0.17
	Median	0.15	0.30	0.41	0.50	0.69	0.38	0.40	0.08	0.16	0.23	0.25	0.28	0.25	0.20
	Q3	0.23	0.48	0.56	0.70	1.07	0.61	0.78	0.13	0.23	0.27	0.33	0.35	0.28	0.25
FeO (%)	Q1	4.51	3.96	3.89	3.45	3.82	4.18	3.74	4.46	2.51	4.91	4.52	3.08	2.60	3.70
	Median	9.52	5.71	5.07	4.10	6.17	5.24	5.23	7.79	3.97	6.04	5.69	4.88	3.23	6.85
	Q3	15.88	7.64	6.35	5.48	7.56	5.88	5.94	9.40	6.39	8.46	7.04	6.22	4.09	9.82
Al	Q1	92.8	95.74	96.19	94.95	93.87	94.48	85.24	90.07	94.45	95.86	95.38	95.23	96.12	96.7
	Median	95.01	96.68	96.86	96.63	95.43	96.06	96.6	93.53	95.74	96.4	96.08	96.06	96.81	96.94
	Q3	96.53	97.16	97.33	97.19	96.62	96.65	97.2	96.71	96.66	97.11	96.64	97	97.22	97.13
CCPl	Q1	62.19	48.01	43.74	39.45	46.75	46.23	40.5	64.87	38.83	42.6	48.02	35.74	36.57	47.43
	Median	84.77	59.02	51.52	47.76	54.89	58.51	50.02	77.03	51.49	53.65	54.45	50.48	40.79	58.62
	Q3	97.6	69.19	58	56.04	59.8	61.77	53.05	89.91	64.37	64.69	60.51	59.2	54.32	71.92

[a] Q1 = first quartile; Q3 = third quartile.

added specifically by alterations contemporaneous with mineralization may be identified by integrating the conclusions drawn from the deposit-scale and detailed-scale studies. By comparing the MPCs with their adjacent host rocks, we interpreted that Au, Cu, Pb, As, Hg and Co were deposited preferentially in the MPCs; in addition, these are some of the elements that experienced gains in the host rocks during alteration phase 2, which included Au-mineralization. Besides, in some minerals in the veins, Au shows positive correlations with Cu, Pb and As. Therefore, Au, Cu, Pb, As, Hg and Co were likely deposited during the mineralizing process in the veins and host rocks. This suggests that a relative increase in the concentrations of Au, Cu, Pb and As, and probably Hg and Co, are good indicators of

Table 3
Median concentrations, and percentage of samples with element concentrations below detection limit (DL) in weakly oxidized mineralized paleo-conduits and their immediate host-rocks, for elements that show concentrations below DL in >15% of the samples of the mineralized zone (not included in Table 2).

Elements	Median concentration (ppm)		% BDL[a]	
	HR ($n=435$)	MPC ($n=97$)	HR[b]	MPC[c]
Ag	0.8	36	30	3
Sb	6	21	36	7
Bi	3	107	35	3
Mo	2	2	23	21
W	10	30	37	22
Cr	7	6	2	3
Cd	2.2	3	25	9

[a] % BDL: percentage of samples with values below detection limit.
[b] HR: host-rock dominated materials (interval 1–10 m).
[c] MPC: mineralized paleo-conduits dominated materials (interval = 0 m).

mineralized zones, even if the hydrothermal alterations and protolith are slightly different from those in the study area.

In deposit-scale exploration, when geochemical data from ground surface or close to it are evaluated, the effects of weathering should be considered. If samples are collected from strongly oxidized parts of the profile, Au, Hg, V, P, Cr, Ni, Be, CaO, Ba and CCPI can be useful indicators of mineralized zones because they are not considerably affected by weathering. Copper, As and FeO can also be used as indicators, but one must be cautious with them because they are more affected by weathering than the elements mentioned above. In contrast, Co, Mn, Pb, Zn and MgO should not be used because their concentrations may be strongly modified by weathering in the upper part of the ground profile.

In the La Josefina and in other deposits under similar conditions as the study area, the models of compositional variation can be used for subsurface and surface exploration of relatively well-known zones, when the mineralized target is expected to be close to the sampled areas. In subsurface exploration, after drilling and analysing the drill core samples, the determination of compositional drifts along boreholes may suggest the presence of and proximity to mineralized veins located beyond the borders of the investigated area. The elements with strongest compositional drifts would be the best to indicate proximity to mineralized rocks. The compositional drifts can also be useful during surface exploration when relatively detailed work (e.g., by trenching) is carried out. However, it is probably in the subsurface where the models are more applicable because of the detailed character of the surveys and the absence of weathering.

Because of weathering, some elements decreased their potential as indicators of proximity to MPCs in the study area, while others become unsuitable indicators. In the strongly oxidized rocks, concentrations of Au, Cu, P, Ba, Hg, K_2O, As, Al_2O_3 and Mn show compositional drifts with shorter ranges (20 or 30 m) than in the weakly oxidized rocks (Table 4; Fig. 8). Concentrations of Na_2O, FeO, V and Ni did not show compositional drifts in strongly oxidized rocks.

The use of several elements together to indicate proximity to MPCs and to differentiate between mineralized and non-mineralized zones is beneficial compared to the use of only the best indicator. Gold is probably the best indicator for Au-rich areas, but it has disadvantages like often occurring in low concentrations, showing high variability, and being transported and concentrated by supergene processes, giving the erroneous impression that there is a genetic link with the host rocks and alterations, while there may be only a spatial association. Using several indicators helps to avoid some of the minor changes due to variations in the geological conditions and due to variability in the concentrations of some elements, compensating some of the variations in one element with correct indications from other elements, and finally improving the success in recognizing mineralized areas. In addition, several elements are easier to determine than Au, and some determinations can be done directly in the field, using for instance gamma ray spectrometers for K or portable X-Ray fluorescence devices for various elements.

Table 4
Strengths and ranges of elements that show compositional drifts in weakly oxidized rocks. The range is the distance from mineralized paleo-conduits, up to which the compositional drifts of the median concentration is preserved. Changes in median concentrations between every two consecutive distance intervals along the curves were calculated as percentage of the shorter-range interval. The "strength" is the average of all the percentages of change between pairs of intervals up to the considered range.

Elements	Strength[a]	Maximun Range (m)	
		Weakly oxidized	Strongly oxidized
Au	−57.55	30	20
Cu	−47.80	40	20
Pb	−40.02	40	60
As	−21.28	40	20
Hg	−39.26	40	20
Ba	34.58	30	20
V	14.70	40	No drift
Ni	33.33	20	No drift
P	96.29	40	30
Mn	23.66	40	30
Al_2O_3	3.56	50	30
K_2O	11.73	40	20
Na_2O	10.78	40	No drift
MgO	32.41	40	40
FeO	−15.15	30	No drift
CCPI	−10.00	30	No drift

[a] Strength calculated up to maximum range. Negative values indicate that mean concentration increase towards MPC.

7. Conclusions

For mineral deposits with geological conditions similar to those of the study area, the most effective deposit-scale geochemical indicators of mineralized zones are Au, Cu, Hg, V, Co, Mn, MgO, Cr, Ba and P. Other potential indicators although probably less effective are Pb, Zn, FeO, CCPI, Be, CaO, As and Ni. In addition, it is likely that Cu, Pb, As, Hg and Co were deposited in the mineralized veins and host rocks at La Josefina mainly during the Au mineralization stage. Therefore, Cu, Pb, As, Hg and Co can be used as good indicators of Au-rich zones even if the geological conditions in those zones are slightly different from those observed during this research.

In detail, the variations in concentrations of several elements in the study area are functions of the distance from paleo-conduits of epithermal fluids. In the system of veins and its hanging wall, where argillic and silicic alterations predominate, the concentrations of 15 elements vary continuously with distance from mineralized paleo-conduits although only the compositional drifts of P, Au, Cu, Pb, Hg, Ba and MgO are strong, up to 30 or 40 m. Therefore, these variables are useful indicators of proximity to Au-rich veins for detailed-scale geochemical surveys during drilling.

The general effects of weathering on elemental concentrations in the study area were moderate, but their consequences vary according to the scale and objective of the geochemical survey. At deposit-scale, if the objective is to identify potential Au-mineralized zones of a few hundred of metres wide, the effects of weathering are mild, although they prevent the use of Co, Mn, Pb, Zn and MgO as indicators because their concentrations may be strongly modified. At detailed-scale, if the objective is to estimate proximity to possible Au-rich veins, the effect of weathering is more significant. It can blur the variations of elemental concentrations due to mineralization, turning Na_2O, FeO, V and Ni into unsuitable indicators of proximity to Au-rich veins, and decreasing the usefulness of Au, Cu, P, Ba, Hg, K_2O, As, Al_2O_3 and Mn.

Previous hydrothermal alterations of original rocks likely have strong influence on the subsequent effects of weathering. This would depend on the composition of the hydrothermal alteration

minerals and their susceptibility to be affected by weathering. Therefore, the concepts about effects of weathering developed in areas that have not undergone hydrothermal alteration should not be directly applied in areas surrounding mineralized veins.

Acknowledgements

The Faculty of Geo-Information Science and Earth Observation (ITC) of the University of Twente, Fomicruz S.E. and Cerro Vanguardia S.A., financially supported this study. We thank Cerro Cazador S.A. and Hunt Mining Corp. for the logistical support, the provision of most geochemical data and the permission to publish them. We thank John Carranza, Martin Hale and two anonymous reviewers for their thorough reviews, which resulted in a great improvement of the manuscript.

References

Alperin, M., Echeveste, H., Fernández, R., Bellieni, G., 2007. Análisis estadístico de datos geoquímicos de volcanitas jurásicas del Macizo del Deseado, provincia de Santa Cruz. Revista de la Asociación Geológica Argentina 62, 200–209.

Arribas, A.J., Schalamuk, I.B., de Barrio, R., Fernández, R., Itaya, T., 1996. Edades radimétricas de mineralizaciones epitermales auríferas del Macizo del Deseado, provincia de Santa Cruz, Argentina. XXXIX Congresso Brasileiro de Geología, Salvador, Brasil: Anales, 7, pp. 254–257.

Berger, B.R., Silberman, M.L., 1985. Relationships of trace-element patterns to geology in hot-spring-type precious metal deposits. In: Berger, B.R., Bethke, P.M. (Eds.), Geology and Geochemistry of Epithermal Systems: Society of Economic Geologists: Reviews in Economic Geology, 2, pp. 233–247.

Booden, M.A., Mauk, J.L., Simpson, M.P., 2011. Quantifying metasomatism in epithermal Au–Ag Deposits: a case study from the Waitekauri Area, New Zealand. Econ. Geol. 106, 999–1030.

Carranza, E.J.M., 2011. Analysis and mapping of geochemical anomalies using log ratio-transformed stream sediment data with censored values. J. Geochem. Explor. 110, 167–185.

Cedillo Frey, A., Páez, G., Ruiz, R., Bauluz Lázaro, B., Subías Pérez, I., 2009. Mineralogía de la alteración hidrotermal en el yacimiento epitermal Mina Martha, Macizo del Deseado, Argentina. Rev. Soc. Española de Mineralogía, Macla 11, 57–58.

Chan, L.S., Wong, P.W., Chen, Q.F., 2007. Abundances of radioelements (K, U, Th) in weathered igneous rocks in Hong Kong. J. Geophys. Eng. 4, 285–292.

Chittleborough, D.J., 1991. Indices of weathering for soils and palaeosols formed on silicate rocks. Aust. J. Earth Sci. 38, 115–120.

Cooke, D.R., Simmons, S.F., 2000. Characteristics and genesis of epithermal gold deposits. In: Hagemann, S.G., Brown, P.E. (Eds.), Gold in 2000: Society of Economic Geologists, Reviews in Economic Geology, 13, pp. 221–244.

Corbella, H., 2005. Nuevas determinaciones de edad absoluta para el Grupo Baqueró, Macizo del Deseado, Patagonia Extrandina. XVI Congreso Geologico Argentino, La Plata: Actas, 1, pp. 69–73.

Darce, M., Levi, B., Nyström, J.O., 1991. Chemical changes during alteration of volcanic rocks and gold ore formation, La Libertad, Nicaragua. J. South Amer. Earth Sci. 4, 87–97.

de Barrio, R., Panza, J.L., Nullo, F., 1999. Jurásico y Cretácico del Macizo del Deseado, provincia de Santa Cruz. In: Caminos, R. (Ed.), Instituto de Geología y Recursos Minerales: Geología Argentina, Anales, 29, pp. 511–527.

Duzgoren-Aydin, N.S., Aydin, A., 2009. Distribution of rare earth elements and oxyhydroxide phases within a weathered felsic igneous profile in Hong Kong. J. Asian Earth Sci. 34, 1–9.

Duzgoren-Aydin, N.S., Aydin, A., Malpas, J., 2002. Distribution of clay minerals along a weathered pyroclastic profile, Hong Kong. Catena 50, 17–41.

Echavarría, L.E., Schalamuk, I.B., Etcheverry, R.O., 2005. Geologic and tectonic setting of Deseado Massif epithermal deposits, Argentina, based on El Dorado–Monserrat. J. South Amer. Earth Sci. 19, 415–432.

Fernández, R., Echeveste, H., Tassinari, C., Schalamuk, I., 1999. Rb-Sr age of the La Josefina epithermal mineralization and its relation with host volcanic rocks. Macizo del Deseado, Santa Cruz Province. Argentina. 2° Simposio Sudamericano de Geología Isotópica, Villa Carlos Paz, Córdoba. Actas:462-465.

Gemmell, J.B., 2007. Hydrothermal alteration associated with the Gosowong epithermal Au–Ag deposit, Halmahera, Indonesia: mineralogy, geochemistry, and exploration implications. Econ. Geol. 102, 893–922.

Giacosa, R., Zubia, M., Sánchez, M., Allard, J., 2010. Meso-Cenozoic tectonics of the Southern Patagonian foreland: structural evolution and implications for Au–Ag veins in the Eastern Deseado Region (Santa Cruz, Argentina). J. South Amer. Earth Sci. 30, 134–150.

Gifkins, C., Herrmann, W., Large, R.R., 2005. Altered volcanic rocks: a guide to description and interpretation. Centre for Ore Deposit Research, University of Tasmania, Hobart. 275 pp.

Gonzalez Guillot, M., de Barrio, R., Ganem, F., 2004. Mina Martha: un yacimiento epitermal argentífero en el Macizo del Deseado, provincia de Santa Cruz. Actas 7° Congreso de Mineralogía y Metalogenia, Río Cuarto, pp. 199–204.

Grant, J.A., 1986. The isocon diagram; a simple solution to Gresens' equation for metasomatic alteration. Econ. Geol. 81, 1976–1982.

Gresens, R.L., 1967. Composition–volume relationships of metasomatism. Chem. Geol. 2, 47–65.

Guan, P., Ng, C.W.W., Sun, M., Tang, W., 2001. Weathering indices for rhyolitic tuff and granite in Hong Kong. Eng. Geol. 59, 147–159.

Hayba, D.O., Bethke, P.M., Heald, P., Foley, K.L., 1985. Geologic, mineralogic, and geochemical characteristics of volcanic-hosted epithermal precious-metal deposits. In: Berger, B.R., Bethke, P.M. (Eds.), Geology and Geochemistry of Epithermal Systems: Society of Economic Geologists: Reviews in Economic Geology, 2, pp. 129–167.

Hedenquist, J.W., Arribas, A.R., Gonzalez-Urien, E., 2000. Exploration for epithermal gold deposits. In: Hagemann, S.G., Brown, P.E. (Eds.), Gold in 2000: Society of Economic Geologists, Reviews in Economic Geology, 13, pp. 245–277.

Herrera, P.A., Closs, L.G., Silberman, M.L., 1993. Alteration and geochemical zoning in Bodie Bluff, Bodie mining district, eastern California. J. Geochem. Explor. 48, 259–275.

Ishikawa, Y., Sawaguchi, T., Iwaya, S., Horiuchi, M., 1976. Delineation of prospecting targets for Kuroko deposits based on modes of volcanism of underlying dacite and alteration halos. Min. Geol. 26, 105–117.

John, D.A., 2001. Miocene and early Pliocene epithermal gold-silver deposits in the northern Great Basin, western United States: characteristics, distribution, and relationship to magmatism. Econ. Geol. 96, 1827–1853.

John, D.A., Hofstra, A.H., Fleck, R.J., Brummer, J.E., Saderholm, E.C., 2003. Geologic setting and genesis of the Mule Canyon low-sulfidation epithermal gold-silver deposit, North-Central Nevada. Econ. Geol. 98, 425–463.

Jovic, S., Guido, D.M., Tiberi, P., Schalamuk, I.B., 2004. Cerro León, una variación del modelo epitermal de baja sulfuración del Macizo del Deseado. Actas 7° Congreso de Mineralogía y Metalogenia, Río Cuarto, Argentina, pp. 225–230.

Jovic, S., Guido, D., Schalamuk, I., Ríos, F., Tassinari, C., Recio, C., 2011. Pingüino In-bearing polymetallic vein deposit, Deseado Massif, Patagonia, Argentina: characteristics of mineralization and ore-forming fluids. Miner. Deposita 46, 257–271.

Large, R.R., Gemmell, J.B., Paulick, H., Huston, D.L., 2001. The alteration box plot: a simple approach to understanding the relationship between alteration mineralogy and lithogeochemistry associated with volcanic-hosted massive sulfide deposits. Econ. Geol. 96, 957–971.

Levinson, A.A., 1974. Introduction to Exploration Geochemistry. Applied Publishing Ltd., Calgary. 612 pp.

Malpas, J., Duzgoren-Aydin, N.S., Aydin, A., 2001. Behaviour of chemical elements during weathering of pyroclastic rocks, Hong Kong. Environ. Int. 26, 359–368.

Mauk, J.L., Simpson, M.P., 2007. Geochemistry and stable isotope composition of altered rocks at the Golden Cross epithermal Au–Ag deposit, New Zealand. Econ. Geol. 102, 841–871.

Moreira, P., 2005. Geología y Metalogénesis del Distrito La Josefina, Macizo del Deseado, Provincia de Santa Cruz. Tesis Doctoral. Facultad de Ciencias Naturales y Museo, Universidad Nacional de La Plata, pp. 383.

Moreira, P., Fernández, R., Mondelo, R., Etcheverry, R., 2002a. Características mineralógicas del sector "Veta Norte". Distrito La Josefina. Provincia de Santa Cruz. Actas VI Congreso de Mineralogía y Metalogenia, Buenos Aires, pp. 271–277.

Moreira, P., Fernández, R., Schalamuk, I., Etcheverry, R., 2002b. Depósitos carbonaticos de hotspring relacionados a manifestaciones epitermales (Au–Ag), distrito La Josefina, Macizo del Deseado, Provincia de Santa Cruz. XV Congreso Geologico Argentino, El Calafate.

Moreira, P., Fernández, R., Ríos, J., Schalamuk, I.A., 2004a. Caracterización de la esfalerita de las manifestaciones epitermales del area La Josefina, Macizo del Deseado, Provincia de Santa Cruz. Actas VII Congreso de Mineralogía y Metalogenia, Río Cuarto (Córdoba), pp. 89–94.

Moreira, P., López, K., Etcheverry, R., Fernández, R., 2004b. Caracterización de la argilización asociada a las manifestaciones epitermales de Au–Ag del área La Josefina, Macizo del Deseado, Santa Cruz. 7° Congreso de Mineralogía y Metalogenia, Río Cuarto, pp. 249–254.

Moreira, P., Fernández, R.R., Schalamuk, I.A., Etcheverry, R.O., Rolando, A.P., 2005. Jurassic magmatism and Au–Ag mineralization in the Deseado Massif (Patagonia Argentina): lead and sulfur isotopic studies. In: Mao, J., Bierlein, F.P. (Eds.), Mineral Deposit Research: Meeting the Global Challenge. Springer, Berlin Heidelberg, pp. 801–804.

Moreira, P., Fernández, R., Cabana, C., Schalamuk, I., 2008. Análisis estructural de las mineralizaciones jurásicas del proyecto epitermal La Josefina (Au–Ag), Macizo del Deseado, Santa Cruz. Revista de la Asociación Geológica Argentina 63, 244–253.

Moreira, P., Echeveste, H., Fernández, R., Hartmann, L.A., Santos, J.O.S., Schalamuk, I., 2009. Depositional age of Jurassic epithermal gold-silver ore in the Deseado Massif, Patagonia, Argentina, based on Manantial Espejo and La Josefina prospects. Neues Jahrbuch für Geologie und Paläontologie - Abhandlungen 253, 25–40.

Murakami, H., Feebrey, C.A., 2001. Geology and geophysical expression of the Yamagano low-sulfidation epithermal Au–Ag deposit, Southwest Kyushu, Japan. In: Feebrey, C.A., Hayashi, T., Taguchi, S. (Eds.), Epithermal Gold Mineralization and Modern Analogues, Kyushu, Japan. Guidebook Series. Society of Economic Geologists, pp. 31–47.

Páez, G.N., Ruiz, R., Guido, D.M., Jovic, S.M., Schalamuk, I.B., 2010. The effects of K-metasomatism in the Bahía Laura Volcanic Complex, Deseado Massif, Argentina: petrologic and metallogenic consequences. Chem. Geol. 273, 300–313.

Pankhurst, R.J., Leat, P.T., Sruoga, P., Rapela, C.W., Márquez, M., Storey, B.C., Riley, T.R., 1998. The Chon Aike province of Patagonia and related rocks in West Antarctica: a silicic large igneous province. J. Volcanol. Geotherm. Res. 81, 113–136.

Panza, J.L., 1998. Hoja Geológica 4769-IV Monumento Nacional Bosques Petrificados, escala 1:250.000, Santa Cruz. Servicio Geológico Minero Argentino: Boletín, 257.

Panza, J.L., Franchi, M., 2002. Magmatismo basáltico cenozoico extrandino. In: Haller, M.J. (Ed.), Relatorio del XV Congreso Geológico Argentino: Geología y recursos naturales de Santa Cruz. Asociación Geológica Argentina, El Calafate, Argentina, pp. 201–236.

Panza, J.L., Haller, M.J., 2002. El volcanismo Jurásico. In: Haller, M.J. (Ed.), Relatorio del XV Congreso Geológico Argentino: Geología y Recursos Naturales de Santa Cruz. Asociación Geológica Argentina, El Calafate, Argentina, pp. 89–102.

Peñalva, G.A., Moreira, P., Chernicoff, C.J., 2005. Área La Josefina, Macizo del Deseado, Provincia de Santa Cruz: nuevas evidencias geofísicas y geoquímicas. XVI Congreso Geológico Argentino, Actas 2, La Plata Actas 2, pp. 807–814.

Pirajno, F., 1992. Hydrothermal mineral deposits: principles and fundamental concepts for the exploration geologist. Springer-Verlag, Berlin. 709 pp.

Ramos, V.A., 2002. Evolución tectónica. In: Haller, M.J. (Ed.), Relatorio del XV Congreso Geológico Argentino: Geología y Recursos Naturales de Santa Cruz. Asociación Geológica Argentina, El Calafate, pp. 1–23.

Reimann, C., Filzmoser, P., 2000. Normal and lognormal data distribution in geochemistry: death of a myth. Consequences for the statistical treatment of geochemical and environmental data. Environ. Geol. 39, 1001–1014.

Rios, F.J., Alves, J.V., Fuzikawa, K., Schalamuk, I.A., de Barrio, R., del Blanco, M., 2000. Fluid evolution in the La Josefina Au-epithermal system, Macizo del Deseado, Southern Patagonia, Santa Cruz, Argentina. Revista Brasileña de Geociencias 30, 769–774.

Schalamuk, I.A., Del Blanco, M.A., de Barrio, R.E., Etcheverry, R.O., Marchionni, D.S., Tesone, M.O., 1998. Características mineralógicas de la paragénesis epitermal del prospecto La Josefina, Macizo del Deseado, Provincia de Santa Cruz. IV Reunión de Mineralogía y Metalogenia, Bahía Blanca, Argentina, pp. 259–266.

Schalamuk, I.B., de Barrio, R.E., Zubia, M., Genini, A., Echeveste, H., 1999. Provincia auroargentífera del Deseado, Santa Cruz. In: Zappettini, E. (Ed.), Recursos Minerales de la República Argentina. Instituto de Geología y Recursos Minerales, SEGEMAR, pp. 1178–1188.

Schalamuk, I.B., de Barrio, R.E., Zubia, M.A., Genini, A., Valvano, J., 2002. Mineralizaciones auroargentíferas del Macizo del Deseado y su encuadre metalogénico, Provincia de Santa Cruz. In: Haller, M.J. (Ed.), Relatorio del XV Congreso Geológico Argentino. El Calafate Asociación Geológica, Argentina, pp. 679–713.

Scott, K.M., 2001. Weathering in the Parkinson Pit and its implications for exploration in the Mt Magnet Mining District, Western Australia. Geochem. Explor. Environ. Anal. 1, 341–352.

Selby, M.J., 1993. Hillslope Materials and Process. Oxford University Press, New York.

Silberman, M.L., Berger, B.R., 1985. Relationships of trace element patterns to alteration and morphology in epithermal precious metal deposits. In: Berger, B.R., Bethke, P.M. (Eds.), Geology and Geochemistry of Epithermal Systems: Society of Economic Geologists: Reviews in Economic Geology, 2, pp. 203–232.

Warren, I., Simmons, S.F., Mauk, J.L., 2007. Whole-rock geochemical techniques for evaluating hydrothermal alteration, mass changes, and compositional gradients associated with epithermal Au–Ag mineralization. Econ. Geol. 102, 923–948.

Zhai, W., Sun, X., Sun, W., Su, L., He, X., Wu, Y., 2009. Geology, geochemistry, and genesis of Axi: a Paleozoic low-sulfidation type epithermal gold deposit in Xinjiang, China. Ore Geol. Rev. 36, 265–281.